92-83-762
MOTC-IOT-91-HA12

240

www.iot.gov.tw

(02)23496789

(　)　　　　　　　110

100

• 　　(02)23496880
61　　4　•　　　(02)23617511
386　　4　•　　(02)25006600
10　　B1•　　(02)25787542
6　•　　(04)22260330
5　•　　　(04)7252792
141　　3　•　　　(07)3324910

GPN　1009202114

0.05　　　　　　　　　　Unluata & Mei (1973)　Mei (1983)

Unluata & Mei (1973)　Mei (1983)

92　6	50	100	

I

TITLE: **The Wave Field near the Head of a Breakwater**

ISBN(OR ISSN)	GOVERNMENT PUBLICATIONS NUMBER 1009202114	IOT SERIAL NUMBER 92-83-762	PROJECT NUMBER 91-HA12

DIVISION: CENTER OF HARBOR & MARINE TECHNOLOGY DIVISION CHIEF: Yung-Fang Chiu PRINCIPAL INVESTIGATOR: Jinn-Hwa Shyu PHONE: 886-4-26587182 FAX: 886-4-26571329	PROJECT PERIOD FROM Jan. 2002 TO Dec. 2002

KEY WORDS: **harbour resonance, sequential condensation process, multizone boundary element method, fundamental standing wave**

ABSTRACT:

   A sequential condensation process combined with the multizone boundary element method is developed to make the numerical computations in a large domain possible for calculation of the harbour oscillations excited by a regular progressive edge wave train. While this technique permits solution for complex topography in and near the harbour, numerical results have been calculated for rectangular harbours of constant depth open to a plane sloping beach with a vertical seawall and connected to a horizontal shelf. In these calculations, the slope of the beach is as small as 0.05 so that a favorable comparison can be made with the analytical solution derived by Unluata & Mei (1973) and Mei (1983) for the case of uniform water depth. In each of these two kinds of solutions, there exists a physical parameter which can describe the radiated waves from the harbour entrance with a definite meaning. By using these parameters, a fundamental standing wave inside the harbour has been found and the physical parameter in each kind of solutions can be shown to be linearly proportional to the amplitude of the difference between the overall standing wave and the fundamental one inside the harbour, suggesting that the harbour resonances are not due to the reinforcement of the energy trapping by harbours, but due to an increase of the incoming and outgoing energy fluxes through the entrance. This situation has become even clearer by further examination of the solution of Unluata & Mei (1973) and Mei (1983), which indicates that except the fundamental standing wave, no significant amount of energy inside a rectangular harbour can be partially reflected by the sudden widening at the entrance.

DATE OF PUBLICATION June 2003	NUMBER OF PAGES 50	PRICE 100	CLASSIFICATION SECRET CONFIDENTIAL UNCLASSIFIED

The views expressed in this publication are not necessarily those of the Ministry of Transportation and Communications.

CONTENTS

CONTENTS OF FIGURE

1. Introduction

It is well known that a harbour or any partially enclosed basin is subject to frequency-dependent oscillations when excited by incident waves of equal frequency through the entrance. For certain frequencies, the amplitudes of these oscillations may be far greater than those of the incident waves, representing a resonant phenomenon. This phenomenon has successfully been predicted by many analytical and numerical models often tested by laboratory experiments. A thorough account on this subject, including an extensive list of the literature, has been given by Mei (1983).

Although, as pointed out by Mei & Agnon (1989), effective numerical techniques now exist and are used in practice to reliably estimate the long-period (several minutes to an hour) oscillations in a harbour induced by incident waves of equal period, the physical mechanism of the harbour resonances occurring in this case remains unclear. For example, even for a simple rectangular harbour, when the resonances occur, it is unclear whether the very large amount of energy inside the harbour is due to energy trapping by the harbour or due to large incoming and outgoing energy fluxes through the entrance. The latter, if it occurs, cannot be seen by inspection of the water surface oscillations in the vicinity of the harbour entrance because of the existence of a node of a standing wave in this region in the event of harbour resonances. On the other hand, the energy trapping by a rectangular harbour with unconstricted mouth owing to the partial reflection of the waves within the harbour by the sudden widening at the entrance has not been proved directly by any mathematical or experimental means. In this study, an effort will be made to clarify the linear mechanism of the harbour resonances occurring in a rectangular harbour induced by incident waves through the entrance, which may have implications for more general situations.

The difficulties mentioned above can be overcome by estimates of the amplitudes of the radiated waves emanating from the harbour entrance. Since the radiated wave function is defined as the difference between the true wave field outside the harbour and that considered to exist as if the harbour entrance were closed, this function includes the difference between the real reflected wave due to the coast with the presence of the harbour entrance and that with the harbour entrance being closed, which arises because of some of the incident wave energy being diffracted through the entrance into the harbour. Therefore, in a general situation, the incoming and outgoing energy fluxes through the entrance cannot be distinguished in this function. However, when the incident wave is a regular progressive edge wave train propagating along a straight coast, since there exists no reflected wave by the coast, the radiated waves propagating along the coast and in the direction opposite to

the incident edge wave can be expected to comprise only the waves truly emanating from the harbour entrance. This outgoing energy subject to reflection and refraction will eventually become edge waves in the region far from the entrance (and on the sloping beach), beyond which not much change in the amplitude will occur. Therefore this amplitude can meaningfully and accurately be related to the oscillations inside the harbour.

When a regular progressive edge wave train is under consideration, an infinitely long sloping beach should be assumed in the simulation. On the other hand, the aim to estimate the amplitude of the radiated edge waves will render some artificial devices in the numerical computations such as fictitious damping inapplicable. Therefore in this study, a large domain is required for the conditions at infinity being satisfied at the outer boundary of this domain (see, for example, Mei 1978). In this large domain, in order to save computer storage space, the overall region is broken up into many portions (referred to as zones), after which a condensation process will be performed to reduce the size of the mathematical model in each zone. In order to obtain a unique solution, these individual condensed equations will be put together by consideration of the continuity conditions on the interfaces between zones. Since the boundary element method, when applied to each zone, can model the interfaces and the conditions on the interfaces very naturally, the condensation process has been utilized to advantage in the multizone boundary element analysis (Kane 1994). The latter however cannot be applied to the solution of the two-dimensional mild-slope or shallow-water equation so that even though the shallow-water approximation is applicable, the three-dimensional Laplace equation will be solved here. To save even more computer memory, a *sequential* condensation process will further be developed and implemented, by which it is unnecessary to put all the condensed equations together at the same time so that a final oversize equation can also be avoided.

Since near the shoreline, the edge waves may dominate in the frequency band between 0.006 and 0.025 Hz according to the field observations by Huntley, Guza & Thornton (1981), and since many harbours may actually resonate at a frequency in this band, the numerical techniques for the solutions of harbour oscillations induced by edge waves are important not only for scientific research but also for engineering applications. Therefore in §2 a general formulation is made for this problem so that the numerical method developed in §3 permits solution for any complex topography in and near the harbour.

After the general theory has been developed, the problems with simple topography will actually be solved in §5 to investigate the mechanism of the harbour resonances. The topography under consideration is a rectangular harbour of constant depth open to a plane

2

sloping beach with a vertical seawall and connected to a horizontal shelf. In this case, the profile and the dispersion relation of the edge waves on this beach can be determined analytically in §4 by using an approach paralleling that of Eckart (1951), Mei (1983), Green (1986), Neu & Oh (1987) and Schäffer & Jonsson (1992). The results will then be applied to the numerical computations in §5 for the solutions of the oscillations inside and outside the harbour induced by these edge waves.

Since in the present computations, the slope of the beach is as small as 0.05 and on the other hand, according to Miles & Munk (1961), the response of a narrow harbour to the incident waves is independent of the angle of incidence, the present numerical solutions, after a convergence test, are compared with the analytical solution derived by Ünlüata & Mei (1973) and Mei (1983) for the case of uniform water depth and normal incidence. The results can both indicate the accuracy of the present numerical model and bear witness to the soundness of the previous analytical theory. Furthermore, in the present numerical solutions, the radiated waves in the region far away from the harbour and on the sloping beach can indeed be shown to have a profile of edge waves.

The amplitudes of these radiated edge waves will in §6 be related to the oscillations inside the harbour, which indicates that for certain lengths of the harbour, a fundamental standing wave inside the harbour can coexist with the incident edge wave without disturbing the latter (meaning that in this situation no radiated waves occur). For other lengths of the harbour, the radiated edge waves arise and their amplitude can be found to be linearly proportional to that of the difference between the overall standing wave and the fundamental one inside the harbour. Since the amplitude of the fundamental standing wave inside the harbour is fixed and equal to that of the incident wave, the above linear relationship suggests that the harbour resonances are due to an increase of the incoming and outgoing energy fluxes through the entrance.

The above phenomena can also be seen in Ünlüata & Mei's (1973) and Mei's (1983) solution, in which the amplitude of the discharge rate per unit depth at the harbour entrance $|Q|$ was derived, which can replace the amplitude of the radiated edge wave in the present discussion. Furthermore, since this analytical solution is in closed form and the quantity $|Q|$, unlike the amplitude of the radiated edge waves, can describes the total discharge at the entrance, this solution can demonstrate that in a steady state, except the fundamental standing wave, no significant amount of energy inside the harbour can be partially reflected by the sudden widening at the entrance. Therefore, the resonances of a narrow rectangular harbour excited by the incident waves through the entrance are indeed due to a drastic increase of the incoming and outgoing energy fluxes through the entrance.

2. Formulation for the problem of harbour oscillations induced by edge waves

Assuming that the fluid is inviscid, incompressible, and irrotational, there exists a velocity potential $\phi(x, y, z, t)$ which satisfies the Laplace equation

$$\nabla^2\phi = \frac{\partial^2\phi}{\partial x^2} + \frac{\partial^2\phi}{\partial y^2} + \frac{\partial^2\phi}{\partial z^2} = 0 \tag{2.1}$$

everywhere in the fluid. We further assume that the waves are of small amplitude at each point. Thus the kinematical and dynamical free-surface conditions become

$$\frac{\partial\zeta}{\partial t} = \frac{\partial\phi}{\partial z} \qquad \text{and} \qquad \frac{\partial\phi}{\partial t} + g\zeta = 0 \qquad \text{at} \qquad z = 0 \tag{2.2}$$

respectively, where ζ is the surface displacement, g the gravitational acceleration, and $z = 0$ corresponds to the mean water level.

Since the incident waves are monochromatic edge waves and only the steady state excitation by these waves is of concern here, the linear solutions of ϕ and ζ at each point are simple harmonic functions with the same frequency ω as the incident waves. Therefore the two free-surface conditions in (2.2) can be combined into

$$\frac{\partial\phi}{\partial z} = \frac{\omega^2}{g}\phi \qquad \text{at} \qquad z = 0 \tag{2.3}$$

On the other hand, the no-flux condition

$$\partial\phi/\partial n = 0 \tag{2.4}$$

is chosen as the condition on any rigid boundary surface, including those at the seawall and seabed.

To determine the conditions at the outer boundary of a large but finite domain, the function ϕ in the region outside the harbour is conveniently expressed as

$$\phi = \phi_i + \phi_d, \tag{2.5}$$

where ϕ_i represents the incident edge wave function and ϕ_d the disturbance or the radiated wave function due to the presence of the harbour and any other deviations from the simple topography on which ϕ_i is considered to occur. Since ϕ_i satisfies the Laplace equation (2.1), ϕ_d will also satisfy this linear and homogeneous equation. Similarly, we have

$$\frac{\partial\phi_d}{\partial z} = \frac{\omega^2}{g}\phi_d \qquad \text{at} \qquad z = 0 \tag{2.6}$$

4

in view of (2.3).

Since in the regions far away from the harbour, the deviation of the actual topography from the simple topography usually has little effect on the solution in and near the harbour, simple topography with a straight coast and a uniform sloping beach can be chosen in the regions far away from the harbour (see figure 1). On this simple one-dimensional topography, the incident edge wave function ϕ_i can be determined analytically (see §4) or by a very simple numerical computation, which satisfies $\partial\phi_i/\partial n = 0$ at the seawall and bottom. Therefore in this region and at the seawall and bottom, we also have

$$\partial\phi_d/\partial n = 0 \qquad (2.7)$$

However, near the harbour, if the natural topography or the breakwater protrudes seaward as shown in figure 1, the disturbance ϕ_d in this region (and therefore the oscillations in the harbour) may alter significantly. Therefore these protrusions must be taken into account, and at their boundaries the condition for ϕ_d is

$$\partial\phi_d/\partial n = -\partial\phi_i/\partial n \qquad (2.8)$$

in view of (2.4) and (2.5). Note that the incident edge wave function ϕ_i in (2.8) is the same function as that determined on the one-dimensional topography according to the definition of ϕ_d. Thus the boundary condition (2.8) is indeed applicable to the solution of ϕ_d.

Also in the vicinity of the harbour, there may exist inlet or bay which can also affect the oscillations in and near the harbour. In these inlet and bay as well as in the harbour, the total velocity potential ϕ will be solved numerically using the field equation (2.1) and the boundary conditions (2.3) and (2.4). Furthermore, to obtain a unique solution, the following continuity conditions on the interface $\overline{AB}$ in figure 1 must be fulfilled:

$$\phi\Big|_{x=0^-} = \phi_i\Big|_{x=0^+} + \phi_d\Big|_{x=0^+} \qquad (2.9)$$

$$\frac{\partial\phi}{\partial n}\Big|_{x=0^-} = \frac{\partial\phi_i}{\partial n}\Big|_{x=0^+} + \frac{\partial\phi_d}{\partial n}\Big|_{x=0^+} \qquad (2.10)$$

Recall that $(\partial\phi_i/\partial n)|_{x=0^+} = 0$, therefore (2.10) can be reduced to

$$\frac{\partial\phi}{\partial n}\Big|_{x=0^-} = \frac{\partial\phi_d}{\partial n}\Big|_{x=0^+}. \qquad (2.11)$$

The above relations have provided all the conditions on the interior boundaries for ϕ and ϕ_d in the regions inside and outside the harbour respectively. We next proceed to

consider the conditions at infinity for ϕ_d, which in a numerical computation will be applied to the outer boundaries of a large domain. For the sake of definiteness, it is assumed that the incident edge wave train propagates in the y direction in figure 1. Also we assume that the sloping beach is connected to a horizontal shelf which then extends to infinity in the x direction. Therefore at infinity from the harbour, except in the regions on or very near the sloping beach, the disturbance ϕ_d contains only the waves of leaky modes, and in the situation illustrated in figure 1, most of these leakages from the sloping beach occur in the region not very far from the harbour entrance. Thus, at infinity but not on the sloping beach, ϕ_d is outgoing and fulfills the Sommerfeld radiation condition

$$(k_d r)^{1/2} \left(\frac{\partial}{\partial r} - i k_d \right) \phi_d \to 0 \quad \text{when} \quad k_d r \to \infty, \tag{2.12}$$

where (r, θ) represent the polar coordinates in figure 1 and k_d the magnitude of the wave-number on the horizontal shelf. Consequently, in practical applications, one may simply impose the condition

$$\frac{\partial \phi_d}{\partial n} \approx \frac{\partial \phi_d}{\partial r} \frac{\partial r}{\partial n} \approx i k_d \phi_d \frac{\partial r}{\partial n} \tag{2.13}$$

at the outer boundaries on the horizontal shelf.

Contrarily, at infinity and on the sloping beach, only the edge waves of all possible modes can exist and their amplitudes will remain unchanged. Therefore, for $y \to \infty$, the disturbance ϕ_d on the sloping beach can be written as

$$\phi_d = e^{-i\omega t} \sum_{j=1}^{m} a_j \psi_j(x, z) e^{i k_{yj} y}, \tag{2.14}$$

where k_{yj} represents the alongshore wave-number of the edge waves of mode j, $\psi_j(x, z)$ represents the distribution in the $x-$ and $z-$directions of the velocity potential of this edge wave mode, and a_j its complex amplitude. In (2.14), the function $\psi_j(x, z)$ and the dispersion relation for determination of k_{yj} in terms of ω, as well as the number of possible modes m on the one-dimensional topography can be determined analytically or by a simple numerical computation. By using these results and considering a group of m points at which the expression (2.14) is valid, one may obtain

$$\left\{ \phi_d \right\} = \left[C \right] \left\{ a \right\}, \tag{2.15}$$

where the components of the column vector $\{\phi_d\}$ are the values of ϕ_d at these m points, the components of $\{a\}$ are a_1, a_2, ..., a_m in (2.14), and the square matrix $[C]$ is determined

by substituting the coordinates (x, y, z) of the m points into the functions $\psi_j(x,z)e^{ik_{yj}y}$ for $j = 1, 2, \ldots, m$.

Since it follows from (2.14) that

$$\frac{\partial \phi_d}{\partial y} = e^{-i\omega t} \sum_{j=1}^{m} i a_j k_{yj} \psi_j(x,z)e^{ik_{yj}y},$$

one can similarly obtain

$$\left\{ \frac{\partial \phi_d}{\partial y} \right\} = \left[D \right] \left\{ a \right\}, \tag{2.16}$$

where $[D]$ is determined from the functions $ik_{yj}\psi_j(x,z)e^{ik_{yj}y}$, $j = 1, 2, \ldots, m$ instead. Therefore, although the column vector $\{a\}$ is unknown, from (2.15) and (2.16) we still have

$$\left\{ \frac{\partial \phi_d}{\partial y} \right\} = \left[D \right] \left[C \right]^{-1} \left\{ \phi_d \right\} \tag{2.17}$$

which can serve as the condition for $y \to \infty$ and on the sloping beach, so that it is satisfied approximately at the corresponding outer boundary of a large domain.

Notice that in (2.14) the edge wave component with the same mode as the incident edge wave may actually represent a deficiency of the latter owing to its diffraction into the harbour, but the phase of this component still propagates in the y direction. Therefore there is no ambiguity in the sign of k_{yj} in (2.14).

On the other hand, when $y \to -\infty$, all the components of ϕ_d propagate in the negative y-direction, so that we have

$$\phi_d = e^{-i\omega t} \sum_{j=1}^{m} b_j \psi_j(x,z)e^{-ik_{yj}y}, \tag{2.18}$$

definitely. From (2.18) one can similarly obtain the approximate boundary condition at $y \sim -\infty$ and on the sloping beach, which takes exactly the same form as (2.17).

3. Numerical method

In the above formulation, the conditions at infinity are applied to the outer boundaries of a large domain. In this large domain, in order to save computer storage space, the overall region will be broken up into many portions, in each of which a boundary element analysis will be performed, so that the field equation (2.1) should be replaced by an equivalent boundary integral equation.

To derive this boundary integral equation, we consider a closed surface S which encloses a volume V and the Green's identity formula

$$\int_V (b\nabla^2 a - a\nabla^2 b)\, dV = \int_S (b\nabla a \cdot \mathbf{n} - a\nabla b \cdot \mathbf{n})\, dS, \tag{3.1}$$

where a, b are any two scalar functions which are reasonable enough to make the above integrations possible. Now we let $b = \phi$ and

$$a = \phi^* \equiv 1/4\pi r, \qquad r = |\mathbf{x} - \mathbf{d}|, \tag{3.2}$$

where $\mathbf{x}$ denotes the vector of position of each point in the field and $\mathbf{d}$ that of a fixed point. Since $\nabla^2\phi = 0$ and

$$\nabla^2\phi^* = \frac{\partial^2\phi^*}{\partial x^2} + \frac{\partial^2\phi^*}{\partial y^2} + \frac{\partial^2\phi^*}{\partial z^2} = -\delta(\mathbf{x} - \mathbf{d})$$

where $\delta(\mathbf{x} - \mathbf{d})$ is the Dirac delta function with the source at $\mathbf{d}$, substitution yields

$$-c\,\phi(\mathbf{d}) = \frac{1}{4\pi}\int_S \left[\phi\frac{\partial}{\partial n}\left(\frac{1}{r}\right) - \frac{1}{r}\frac{\partial\phi}{\partial n}\right] dS \tag{3.3}$$

where

$$c = \begin{cases} 0, & \mathbf{d} \text{ is outside } S; \\ 1, & \mathbf{d} \text{ is inside } S; \\ \frac{1}{2}, & \mathbf{d} \text{ is on a smooth portion of } S; \\ \frac{\theta}{4\pi}, & \mathbf{d} \text{ is at a sharp corner on } S \text{ with a solid angle } \theta. \end{cases} \tag{3.4}$$

When the source point $\mathbf{d}$ is located precisely on S, the integrand in (3.3) becomes singular at the point $\mathbf{x} = \mathbf{d}$. Therefore the last two relations in (3.4) are achieved when the integral in (3.3) is interpreted in the Cauchy principal-value sense. In this situation, the integral equation (3.3) involves only the values of ϕ and $\partial\phi/\partial n$ on S. Thus, after discretization of (3.3) for each $\mathbf{d}$ collocated at the nodes on S, we have an approximate set of N linear algebraic equations

$$\sum_{j=1}^{N} H_{ij}\phi_j - \sum_{j=1}^{N} G_{ij}\left(\frac{\partial\phi}{\partial n}\right)_j = 0, \qquad i = 1, 2, \ldots, N$$

8

or in matrix notation

$$\left[H\right]\left\{\phi\right\} - \left[G\right]\left\{\frac{\partial\phi}{\partial n}\right\} = 0, \tag{3.5}$$

where ϕ_j and $(\partial\phi/\partial n)_j$ denote the values of ϕ and $\partial\phi/\partial n$ at node j, and the coefficient matrices $[H]$ and $[G]$, including the number of nodes N, depend on the specific details of the discretization process which are not elaborated here.

After the equation (3.5) has been solved, the value of ϕ at any point within S can be recovered by locating the source point **d** at this point and then performing the surface integration in (3.3). However, in the present problem, if the wavelength is very large compared with the water depth, the vertical variation of ϕ is weak so that the calculations of the interior response is usually unnecessary.

Since the disturbance ϕ_d also satisfies the Laplace equation, by the same argument, we also have

$$\left[H_d\right]\left\{\phi_d\right\} - \left[G_d\right]\left\{\frac{\partial\phi_d}{\partial n}\right\} = 0. \tag{3.6}$$

for estimates of the node-point values of ϕ_d and $\partial\phi_d/\partial n$ on a closed surface outside the harbour. Now if the closed surfaces chosen for (3.5) and (3.6) are those which enclose the entire regions inside and outside the harbour respectively in the domain, by using the boundary conditions given in §2, the unknows $\partial\phi/\partial n$ and $\partial\phi_d/\partial n$ at each node on these surfaces, except that on the interface $\overline{AB}$ in figure 1 can be eliminated. Furthermore, by invoking the matching conditions (2.9) and (2.11), the unknowns ϕ and $\partial\phi/\partial n$ at each node on $\overline{AB}$ in (3.5) can also be eliminated in favor of ϕ_d and $\partial\phi_d/\partial n$ at the same node. Nevertheless, equations (3.5) and (3.6) must now be solved simultaneously so that if there exist L nodes in (3.6), combination of (3.5) and (3.6) yields a set of $L + N$ simultaneous linear equations with $L + N$ unknowns, which is nonhomogeneous due to the existence of ϕ_i in (2.9). Thus a unique, nontrivial solution can in theory be obtained by using an equation-solving technique. However, the large domain used here will render the size of this system of equations too large to be dealt with by a computer. Therefore a multizone analysis with sequential condensation is needed.

In the above discussion, the domain has been divided at the harbour entrance into two regions but without condensation. In order to condense (3.5), we reorder its degrees of freedom and partition it into blocks (see Kane 1994):

$$\begin{bmatrix} [H_{MM}] & [H_{MC}] \\ [H_{CM}] & [H_{CC}] \end{bmatrix} \left\{ \begin{array}{c} \{\phi_M\} \\ \{\phi_C\} \end{array} \right\} = \begin{bmatrix} [G_{MM}] & [G_{MC}] \\ [G_{CM}] & [G_{CC}] \end{bmatrix} \left\{ \begin{array}{c} \{(\partial\phi/\partial n)_M\} \\ \{(\partial\phi/\partial n)_C\} \end{array} \right\}, \tag{3.7}$$

9

where $\{\phi_M\}$ and $\{(\partial\phi/\partial n)_M\}$ contain the node-point values of ϕ and $\partial\phi/\partial n$ on the interface $\overline{AB}$ while $\{\phi_C\}$ and $\{(\partial\phi/\partial n)_C\}$ contain those on the remaining boundaries of the body of water in the harbour. Therefore by substituting (2.3) and (2.4) in (3.7) and collecting terms, we obtain

$$
\begin{bmatrix} [H_{MM}] & [H'_{MC}] \\ [H_{CM}] & [H'_{CC}] \end{bmatrix} \begin{Bmatrix} \{\phi_M\} \\ \{\phi_C\} \end{Bmatrix} = \begin{bmatrix} [G_{MM}] & [0] \\ [G_{CM}] & [0] \end{bmatrix} \begin{Bmatrix} \{(\partial\phi/\partial n)_M\} \\ \{0\} \end{Bmatrix}, \qquad (3.8a,b)
$$

where $[H'_{MC}]$, $[H'_{CC}]$ are different from $[H_{MC}]$, $[H_{CC}]$ in (3.7). Solving the matrix equation (3.8b) for $\{\phi_C\}$ gives

$$
\{\phi_C\} = \begin{bmatrix} H'_{CC} \end{bmatrix}^{-1} \left(\begin{bmatrix} G_{CM} \end{bmatrix} \{(\partial\phi/\partial n)_M\} - \begin{bmatrix} H_{CM} \end{bmatrix} \{\phi_M\} \right). \qquad (3.9)
$$

Substitution in (3.8a) for $\{\phi_C\}$ yields

$$
\begin{bmatrix} F \end{bmatrix} \{\phi_M\} = \begin{bmatrix} E \end{bmatrix} \{(\partial\phi/\partial n)_M\}, \qquad (3.10)
$$

where

$$
\begin{bmatrix} F \end{bmatrix} = \begin{bmatrix} H_{MM} \end{bmatrix} - \begin{bmatrix} H'_{MC} \end{bmatrix} \begin{bmatrix} H'_{CC} \end{bmatrix}^{-1} \begin{bmatrix} H_{CM} \end{bmatrix}, \qquad (3.11)
$$

$$
\begin{bmatrix} E \end{bmatrix} = \begin{bmatrix} G_{MM} \end{bmatrix} - \begin{bmatrix} H'_{MC} \end{bmatrix} \begin{bmatrix} H'_{CC} \end{bmatrix}^{-1} \begin{bmatrix} G_{CM} \end{bmatrix}. \qquad (3.12)
$$

In (3.10), the unknown vectors $\{\phi_M\}$ and $\{(\partial\phi/\partial n)_M\}$ contain only the node-point values of ϕ and $\partial\phi/\partial n$ on the interface $\overline{AB}$ in figure 1 so that the size of (3.10) is much smaller than that of (3.5). Therefore equation (3.10) combined with that derived in the region outside the harbour produces a smaller system of equations. Its solution can be substituted in (3.9) to recover $\{\phi_C\}$.

Note that, as pointed out by Kane (1994), the condensation procedure embodied in the above equations is an exact formulation, in which no terms have been neglected, nor has any approximation been made. Therefore this procedure can repeatedly be applied in the region outside the harbour, which is much larger than that in the harbour.

To reduce the size of (3.6) without sacrifice of the grid resolution, the domain outside the harbour is broken up into many portions, referred to as zones, as illustrated in figure 2. Therefore, in zone-1, following the same procedure as that resulting in (3.5) or (3.6), we obtain

$$
\begin{bmatrix} H_d \end{bmatrix}_1 \begin{Bmatrix} \phi_d \end{Bmatrix}_1 - \begin{bmatrix} G_d \end{bmatrix}_1 \begin{Bmatrix} \dfrac{\partial\phi_d}{\partial n} \end{Bmatrix}_1 = 0. \qquad (3.13)
$$

10

where $\{\phi_d\}_1$ and $\{\partial\phi_d/\partial n\}_1$ contain the node-point values of ϕ_d and $\partial\phi_d/\partial n$ on the boundary surface of zone-1. Again, reordering the degrees of freedom and partitioning (3.13) into blocks, we obtain

$$
\begin{bmatrix} \begin{bmatrix} H_{dMM} \end{bmatrix}_1 & \begin{bmatrix} H_{dMC} \end{bmatrix}_1 \\ \begin{bmatrix} H_{dCM} \end{bmatrix}_1 & \begin{bmatrix} H_{dCC} \end{bmatrix}_1 \end{bmatrix} \left\{ \begin{matrix} \{\phi_{dM}\}_1 \\ \{\phi_{dC}\}_1 \end{matrix} \right\} = \begin{bmatrix} \begin{bmatrix} G_{dMM} \end{bmatrix}_1 & \begin{bmatrix} G_{dMC} \end{bmatrix}_1 \\ \begin{bmatrix} G_{dCM} \end{bmatrix}_1 & \begin{bmatrix} G_{dCC} \end{bmatrix}_1 \end{bmatrix} \left\{ \begin{matrix} \{(\partial\phi_d/\partial n)_M\}_1 \\ \{(\partial\phi_d/\partial n)_C\}_1 \end{matrix} \right\}, \quad (3.14)
$$

where $\{\phi_{dM}\}_1$ and $\{(\partial\phi_d/\partial n)_M\}_1$ contain the node-point values of ϕ_d and $\partial\phi_d/\partial n$ on the interface between zone-1 and zone-2, and $\{\phi_{dC}\}_1$ and $\{(\partial\phi_d/\partial n)_C\}_1$ contain those on the remaining boundary surfaces of zone-1 on which the boundary conditions (2.6), (2.7), (2.13) and (2.17) can be applied separately. Therefore the unknowns in $\{(\partial\phi_d/\partial n)_C\}_1$ can also be eliminated entirely from (3.14) in favour of those in $\{\phi_{dC}\}_1$, resulting in

$$
\begin{bmatrix} \begin{bmatrix} H_{dMM} \end{bmatrix}_1 & \begin{bmatrix} H'_{dMC} \end{bmatrix}_1 \\ \begin{bmatrix} H_{dCM} \end{bmatrix}_1 & \begin{bmatrix} H'_{dCC} \end{bmatrix}_1 \end{bmatrix} \left\{ \begin{matrix} \{\phi_{dM}\}_1 \\ \{\phi_{dC}\}_1 \end{matrix} \right\} = \begin{bmatrix} \begin{bmatrix} G_{dMM} \end{bmatrix}_1 & \begin{bmatrix} 0 \end{bmatrix} \\ \begin{bmatrix} G_{dCM} \end{bmatrix}_1 & \begin{bmatrix} 0 \end{bmatrix} \end{bmatrix} \left\{ \begin{matrix} \{(\partial\phi_d/\partial n)_M\}_1 \\ \{0\} \end{matrix} \right\}, \quad (3.15a,b)
$$

Solving (3.15b) for $\{\phi_{dC}\}_1$ gives

$$
\{\phi_{dC}\}_1 = \begin{bmatrix} H'_{dCC} \end{bmatrix}_1^{-1} \left(\begin{bmatrix} G_{dCM} \end{bmatrix}_1 \{(\partial\phi_d/\partial n)_M\}_1 - \begin{bmatrix} H_{dCM} \end{bmatrix}_1 \{\phi_{dM}\}_1 \right). \quad (3.16)
$$

Substitution in (3.15a) for $\{\phi_{dC}\}_1$ yields

$$
\begin{bmatrix} F_d \end{bmatrix}_1 \{\phi_{dM}\}_1 = \begin{bmatrix} E_d \end{bmatrix}_1 \{(\partial\phi_d/\partial n)_M\}_1, \quad (3.17)
$$

where

$$
\begin{bmatrix} F_d \end{bmatrix}_1 = \begin{bmatrix} H_{dMM} \end{bmatrix}_1 - \begin{bmatrix} H'_{dMC} \end{bmatrix}_1 \begin{bmatrix} H'_{dCC} \end{bmatrix}_1^{-1} \begin{bmatrix} H_{dCM} \end{bmatrix}_1, \quad (3.18)
$$

$$
\begin{bmatrix} E_d \end{bmatrix}_1 = \begin{bmatrix} G_{dMM} \end{bmatrix}_1 - \begin{bmatrix} H'_{dMC} \end{bmatrix}_1 \begin{bmatrix} H'_{dCC} \end{bmatrix}_1^{-1} \begin{bmatrix} G_{dCM} \end{bmatrix}_1. \quad (3.19)
$$

The achievement of (3.16)-(3.19) completes the first condensation outside the harbour. Since equation (3.17) can be rewritten as

$$
\{(\partial\phi_d/\partial n)_M\}_1 = \begin{bmatrix} E_d \end{bmatrix}_1^{-1} \begin{bmatrix} F_d \end{bmatrix}_1 \{\phi_{dM}\}_1, \quad (3.20)
$$

it can serve as the boundary condition on the interface between zone-1 and zone-2 for the solution in zone-2. Therefore the above condensation procedure can be repeated in zone-2, and so on, until the numerically generated boundary condition on the interface between

zone-5 and zone-12 in figure 2 is obtained. Similarly, beginning with the condensation in zone-6 and ending with that in zone-10 in figure 2, one can also obtain the numerically generated boundary condition on the interface between zone-10 and zone-12. On the other hand, equation (3.10) together with (2.9) and (2.11) provides another condition on the interface between zone-11 and zone-12. Therefore, by using this sequential condensation process, one can finally obtain a well-imposed boundary-value problem within zone-12 in figure 2 that is much smaller than the actual domain.

After the node-point values of ϕ_d and $\partial\phi_d/\partial n$ on the boundary of zone-12 are determined, the node-point values of ϕ_d and $\partial\phi_d/\partial n$ in other zones, including those of ϕ and $\partial\phi/\partial n$ in the harbour can be recovered by using the equations (3.16)-(3.19) and the similar ones in different zones. This task can however be accomplished in a separate effort so that the entries of the coefficient matrices involved can be stored in a hard disk for later use. Therefore the sequential condensation process can be done *in place*. That is to say, the computer memory used to store the entries of the matrices in one zone can be reused to store those in other zones. Hence, in this approach, the computer memory imposes no restriction on the number of zones, and with less computer memory, smaller zones can be used by breaking up the domain into more portions with various configurations.

4. Edge waves on a sloping beach with a seawall and shelf

After the general formulation and the method of solution have been developed in the previous two sections, a specific situation will be considered in this and the following sections. In this situation, the topography outside the harbour is composed of a plane sloping beach bounded by a vertical wall and connected to a horizontal shelf as shown in figure 3. This topography, if the harbour entrance were closed, is one-dimensional so that the wave profile and the dispersion relation of the incident edge waves can be determined analytically in this section, which are required for the numerical computations in §5.

We note that the vertical wall at the shoreline can avoid the occurrence of the depth discontinuities in the neighborhood of the harbour entrance when a harbour of constant depth is open to this beach. Also, in this situation, the interface between the regions inside and outside the harbour is vertical. All of these will later be proved to be crucial for the solutions being of physical interest. On the other hand, the horizontal shelf in figure 3 is required for the validity of the boundary condition (2.13). In addition, the horizontal shelf can ensure that the water can stay shallow everywhere so that the shallow-water approximation can be applied here. The present analysis parallels that in Eckart (1951), Mei (1983), Green (1986), Neu & Oh (1987), and Schäffer & Jonsson (1992), but is summarized here for completeness.

In linear shallow-water theory, the governing equation is

$$\nabla \cdot (gh\nabla\zeta) - \frac{\partial^2 \zeta}{\partial t^2} = 0 \tag{4.1}$$

(see, for example, Mei 1983), where h represents the water depth at each location. The relation between ζ and ϕ is simply that

$$\phi(x,y,z,t) = -\frac{ig}{\omega}\zeta(x,y,t) \tag{4.2}$$

in view of (2.2) and the fact that in shallow-water approximation, the vertical variation of ϕ is negligible. Restricting ourselves to consider only the solutions which are harmonic in time and in the alongshore (i.e. y) direction, we have

$$\zeta = \eta(x)\exp[i(k_y y - \omega t)]. \tag{4.3}$$

Substitution into (4.1) yields

$$\frac{d}{dx}\left(gh\frac{d\eta}{dx}\right) + (\omega^2 - ghk_y^2)\eta = 0. \tag{4.4}$$

13

This equation will be solved in regions I and II separately and the results will be matched at $x = x_1$ in figure 3.

Let us first consider the situation in region I, in which the beach slope h_x is constant and the water depth

$$h = h_x x \tag{4.5}$$

in accordance with the coordinates shown in figure 3, which are different from those in figure 1. Substituting (4.5) in (4.4), we obtain in region I

$$x\frac{d^2\eta}{dx^2} + \frac{d\eta}{dx} + \left(\frac{\omega^2}{gh_x} - k_y^2 x\right)\eta = 0. \tag{4.6}$$

By the following transformation

$$\xi \equiv 2k_y x, \qquad \eta = \exp(-\xi/2)f(\xi), \tag{4.7}$$

equation (4.6) may be rewritten as

$$\xi\frac{d^2 f}{dx^2} + (1 - \xi)\frac{df}{dx} - a_I f = 0, \tag{4.8}$$

where

$$a_I = -\frac{1}{2}\left(\frac{\omega^2}{gk_y h_x} - 1\right). \tag{4.9}$$

Equation (4.8) belongs to the class of confluent hypergeometric equations (more specifically Kummer's equation, see Abramowitz & Stegun 1972), and its general solution can be written as

$$f = AM(a_I, 1, \xi) + BU(a_I, 1, \xi), \tag{4.10}$$

where M and U are the Kummer function.

We next proceed to find the solution in region II. In this region, the water depth $h = \text{const} = h_1$, so that equation (4.4) reduces to

$$\frac{d^2\eta}{dx^2} + \left(\frac{\omega^2}{gh_1} - k_y^2\right)\eta = 0$$

or

$$\frac{d^2\eta}{dx^2} - \lambda k_y^2 \eta = 0,$$

where

$$\lambda \equiv 1 - \frac{\omega^2}{gh_1 k_y^2}. \tag{4.11}$$

The general solution of (4.11) is

$$\eta = C \exp\left(-\lambda^{\frac{1}{2}} k_y x\right) + D \exp\left(\lambda^{\frac{1}{2}} k_y x\right)$$

or in terms of ξ

$$\eta = C \exp\left(-\lambda^{\frac{1}{2}} \xi/2\right) + D \exp\left(\lambda^{\frac{1}{2}} \xi/2\right). \tag{4.12}$$

If $\lambda < 0$, solution (4.12) together with (4.3) describes two progressive wave trains with the phase velocity $(gh_1)^{1/2}$ as expected. Since the amplitudes of these two wave trains are constant in region II, these waves are not confined to the shoreline and therefore are not edge waves. Thus edge waves can occur only if $\lambda > 0$, signifying that for edge waves, ω can at most attain the value given by $\omega^2 = gh_1 k_y^2$; this value is therefore called the cut-off frequency.

When $\lambda > 0$, the last term in (4.12) gives exponential seaward growth and therefore must be discarded by setting $D = 0$. Thus in region II, we have

$$\eta_{II} = C \exp\left(-\lambda^{\frac{1}{2}} \xi/2\right), \tag{4.13}$$

while in region I, it follows from (4.7) and (4.10) that

$$\eta_I = A \exp(-\xi/2) M(a_I, 1, \xi) + B \exp(-\xi/2) U(a_I, 1, \xi). \tag{4.14}$$

Two of the three coefficients in (4.13) and (4.14) and the parameter a_I which is allied to the dispersion relation through (4.9), can be determined by using the boundary condition $d\eta/dx = \partial\phi/\partial x = 0$ at the seawall (see (4.2)) and the matching conditions $\eta_I = \eta_{II}$ and $(d\eta/dx)_I = (d\eta/dx)_{II}$ at $x = x_1$. As a consequence, a homogeneous system of three linear equations in A, B and C can be established, and to get nontrivial solutions, the determinant of the coefficient matrix of this system must vanish. This adds the constraint on the values of a_I and therefore defines the edge wave dispersion relation for the present topography. The results for a particular situation are shown in figure 4.

Recall that in Eckart's (1951) theory for an infinitely extended plane sloping beach without a seawall, the dispersion relation of the edge waves follows from the requirement that parameter a_I must be a negative integer or zero, $-a_I = n$. Thus, by using (4.9), this relation can be written as

$$\frac{\omega^2 h_0}{gh_x^2} = (2n+1)\frac{k_y h_0}{h_x}, \quad n = 0, 1, 2, \ldots$$

15

Therefore, if it is plotted in figure 4, there will be an infinite number of straight lines, all passing through the origin; each represents the dispersion relation of a certain mode. However, these straight lines have now become curved due to the presence of the seawall. Moreover, the existence of the horizontal shelf can cause a cut-off of not only the frequency but also the number of possible edge wave modes for a fixed ω according to figure 4. Hence the number of modes m in (2.14) is indeed finite.

After the value of k_y for a fixed ω and a fixed mode has been determined, one may compute the values of the coefficients B and C in terms of A by using any two equations in the system of three equations mentioned above, which completes the solution of the edge waves for the present topography. The resulting profile of the fundamental edge wave mode under the circumstances corresponding to the intersection S in figure 4 is shown in figure 5, which indicates that $d\eta/dx$ indeed vanishes at the seawall and the values of η and $d\eta/dx$ are continuous at $x = x_1$.

5. Numerical solutions of harbour oscillations

In this section, we shall compute the oscillations inside and outside a rectangular harbour of constant depth open to the ocean with the topography considered in §4, which are induced by an edge wave train with the frequency and wave-number corresponding to point S in figure 4. In this situation, although the frequency is fixed as $\omega = 2\pi/160$ rad sec^{-1}, by varying the length l and width b of the harbour, the phenomenon of harbour resonances can still be observed in the numerical solutions which will then be compared with the analytical solution derived by Ünlüata & Mei (1973) and Mei (1983).

Since according to figure 4, among the edge waves of period 160 sec, only the fundamental mode can occur in this situation, the condition (2.17) and the corresponding one derived from (2.18) now reduce to

$$\frac{\partial \phi_d}{\partial y} = ik_y \phi_d, \qquad \frac{\partial \phi_d}{\partial y} = -ik_y \phi_d$$

respectively. These conditions, when applied to the boundaries $\overline{AB}$ and $\overline{EF}$ in figure 6, can both be written as

$$\frac{\partial \phi_d}{\partial n} = ik_y \phi_d, \tag{5.1}$$

because the outward normal directions of these two boundaries are opposite to each other. Notice that unlike (2.17), the boundary condition (5.1) as well as the matching condition (2.9) can be applied without knowing the profile of the edge waves in the x direction, so that the solution of the latter derived in §4 will later be utilized for comparison purposes.

The use of a fixed frequency in the present computations can also make the convergence test of the numerical solutions much easier. To achieve this purpose, we calculate the amplification factor R of a harbour with $l = 1.4$ km and $b = 200$ m but with different domain length L in figure 6. The amplification factor R is now defined as the ratio of the amplitude at point P in figure 6 to that at the shoreline of the incident edge waves. The results in figure 7 indicate that after the outer boundaries are taken three wavelengths away from the harbour entrance, further expansion of the domain gives rise to negligible changes of the solution. This conclusion can be applied to the situations with different values of l and b, because as long as the frequency and the topography outside the harbour remain unchanged and the harbour width b is very small compared with L, it can be expected that the condition when the boundary conditions (2.13) and (5.1) can be applied to the outer boundaries accurately should be independent of l and b.

The validity of (2.13) and (5.1) for a large but finite domain as well as the accuracy of the present model can also be checked by comparison of the numerical solution of ϕ_d on the interface between zone-1 and zone-2 in figure 2 with the analytical solution in figure 5. The results in figure 8 indicate that when $k_d L/2\pi = 3.72$ (i.e. $L = 20$ km), the disturbance ϕ_d on the sloping beach and on the interface between zone-1 and zone-2 which in this case is at the distance of 19.8 km from the center of the harbour entrance, can fit the profile of the fundamental edge wave mode very well. Since this profile has never been utilized in the present numerical computations, this fitness indeed provides a valuable check on the validity of (2.13) and (5.1) and on the accuracy of the present model. Furthermore, it also demonstrates that the disturbance ϕ_d in this region contains only the trapped mode edge waves. This situation is general for the value of $k_d L/2\pi$ being larger than 3. Therefore in the following computations we keep $L = 20$ km.

After the domain is decided, we compute the oscillations inside and outside the harbour for different values of l under the situations that $b = 200$ m and $b = 50$ m. Therefore, in figure 9, the amplification factor R varies with l normalized by the wave-number in the harbour $k = \omega/(gh_0)^{1/2}$. These results are certainly not the so-called response curve of a harbour, but can still show the resonant peaks in figures 9a and 9b. In each of these figures, the two resonant peaks virtually have the same height, contrary to the situation of the response curve, in which the height of successive resonant peaks decreases with the node number of resonances (see, for example, Hwang & Tuck 1970; Lee 1971; Mei & Chen 1975).

The above phenomena regarding the height of the resonant peaks can be accounted for by the analytical solution (6.20) in §5.6.2 in Mei (1983) deduced by using the method of matched asymptotic expansions for a narrow rectangular harbour open to the ocean of constant depth (also see Ünlüata & Mei 1973). This solution, in the present notation, can be written as

$$R_c = [\cos kl + (kb/\pi)\sin kl \ln(\gamma kb/\pi e) - i(kb/2)\sin kl]^{-1}, \tag{5.2}$$

where $\ln e = 1$, $\ln \gamma =$ Euler's constant$= 0.5772157\ldots$, and R_c is the complex amplification factor. Thus in this solution

$$R = |R_c| = \left\{ [\cos kl + (kb/\pi)\sin kl \ln(\gamma kb/\pi e)]^2 + [(kb/2)\sin kl]^2 \right\}^{-1/2}. \tag{5.3}$$

From (5.3) it is immediately clear that if $kb =$ constant, the variation of R with kl is periodic with a period of π, so that the occurrences of the resonant peaks will repeat with the same height. In the more complicated situation when both kl and kb vary due to the change of k, a close investigation into (5.2) made by Mei (1983) has shown that the height of successive

18

resonant peaks in the response curve indeed decreases with the mode number (see (6.26) in §5.6.2 in Mei (1983)).

The analytical solution (5.3) for $b = 200$ m and $b = 50$ m has also been plotted in figure 9 for comparison, which indicates that except in the vicinity of the resonant peaks, the present numerical solutions agree well with the analytical solution. This might be attributed to the situation that when $kl \approx \pi$, the term $\cos kl$ in (5.3) is dominant and the other terms in (5.3) which all contain the small parameter kb are then responsible for the value of R being slightly less than 1 when kl is slightly smaller than π; this slight deviation also occurs precisely to the present numerical solutions.

Since solution (5.3) represents matched asymptotics, it will become more accurate when the ordering parameter kb decreases. Therefore the improvement of the agreement between the numerical and analytical solutions in figure 9b for a narrower harbour and the situation that the circles in figure 9 can fit the curves extremely well when $kl \approx \pi$, both imply that the very gentle slope, $h_x = 0.05$, considered here, while allowing for the occurrences of the edge waves, has little effect on the harbor response; the latter for a narrow harbour is also independent of the angle of incidence, in accordance with Miles & Munk's (1961) theory.

6. Discussion

Since the disturbance ϕ_d on the sloping beach and on the interface between zone-1 and zone-2 in figure 2 represents the waves emanating from the harbour entrance and contains only the trapped mode edge waves (see figure 8) which cannot be attenuated by energy spread and leakage, the amplitude of ϕ_d on this interface and at the shoreline (denoted by A_R) will be related to the oscillations inside the harbour, that can eventually provide a physical insight into the mechanism of the harbour resonances.

In figure 10, the abscissa is the amplitude A_P of ϕ at point P in figure 6 normalized by the amplitude of ϕ_i at the shoreline A_0. Since the oscillations inside the harbour in the present calculations are almost a perfect standing wave, the quantity A_P can describe the oscillations inside the harbour in whole. However, from figure 10 it is clear that neither a linear nor an one-to-one relation between A_P and A_R exists. The results in figure 10 also show that $A_P/A_0 = 1$ when A_R vanishes. This and the situation that the event of $A_R = 0$ occurs when $kl = \pi$ (see figure 11) indicate that if the standing wave inside the harbour has an antinode at the entrance, this standing wave after its amplitude reaches the same level as that of the incident edge wave, can coexist with the latter without disturbing it (i.e. $\phi_d = 0$ everywhere). This phenomenon is consistent with the matching conditions (2.9) and (2.10) for a narrow harbour, because in this case, the value of $\phi_i|_{x=0+}$ at the harbour entrance is near uniform and therefore itself can be balanced by $\phi|_{x=0-}$ approximately, while $(\partial\phi/\partial n)|_{x=0-} = (\partial\phi_i/\partial n)|_{x=0+} = 0$ if $kl = \pi$.

The above situation will become even clearer when the incident wave is of normal incidence. This incident wave together with the reflected wave from the seawall forms a standing wave outside the harbour. Therefore, if $kl = n\pi$, $n = 1, 2, 3, \ldots$, the standing waves inside and outside the harbour with the same amplitudes can balance each other exactly. The former will hereafter be referred to as the fundamental standing wave in the harbour.

When $kl \neq n\pi$, the oscillations inside the harbour will change from the fundamental standing wave into a different standing wave to fulfill the no-flux condition (2.4) on the backwall of the harbour which is now at a different distance from the entrance so that the antinode of the overall standing wave may not occur at the entrance (but will always occur on the backwall of the harbour). Consequently, in order to satisfy the conditions (2.9) and (2.10) simultaneously, the disturbance ϕ_d arises outside the harbour, accompanied by a further change of the oscillations inside the harbour. Therefore one may expect that the quantity A_R which describes the disturbance outside the harbour with a definite meaning might be related to the difference between the overall standing wave and the fundamental one in the harbour.

20

Since for different values of kl, the standing wave in the harbour will change in amplitude and phase as well as the locations of antinodes, the difference between the overall standing wave and the fundamental one in the harbour in general cannot be represented by another standing wave, but is composed of two wave trains propagating in opposite directions with different amplitudes. These two wave trains can be estimated as follows.

First, for a certain value of kl and at a certain instant $t = t_0$, if the value of ϕ at point P in figure 6 is $A_P e^{i\beta}$, the overall standing wave within the harbour at this instant can be written as

$$\phi = \frac{A_P}{2} e^{i(\beta + kx + kl)} + \frac{A_P}{2} e^{i(\beta - kx - kl)}. \tag{6.1}$$

in the coordinates shown in figure 1. On the other hand, if $\phi_i = A_0 e^{i\alpha}$ at point O in figure 6 and at $t = t_0$, the fundamental standing wave in the harbour at this instant can be represented approximately as

$$\phi_0 = \frac{A_0}{2} e^{i(\alpha + kx)} + \frac{A_0}{2} e^{i(\alpha - kx)}. \tag{6.2}$$

Therefore, if without loss of generality, the two wave trains representing the difference between the overall standing wave and the fundamental one in the harbour are expressed as

$$\phi_{\text{out}} = B e^{i(\alpha + kx + \theta)}, \quad \phi_{\text{in}} = B' e^{i(\alpha - kx + \theta')}, \tag{6.3}$$

we have

$$B e^{i\theta} = \frac{A_P}{2} e^{i(\beta + kl - \alpha)} - \frac{A_0}{2}, \tag{6.4}$$

$$B' e^{i\theta'} = \frac{A_P}{2} e^{i(\beta - kl - \alpha)} - \frac{A_0}{2}. \tag{6.5}$$

By using (6.4), (6.5) and the given values of A_0 and α as well as the numerical solutions of A_P and β, the amplitudes B and B' (and also the phase shifts θ and θ') can be determined and related to A_R for different values of kl in the cases of $b = 200$ m and $b = 50$ m. The results in figure 12 show that the amplitudes of these additional oscillations inside the harbour are indeed linearly proportional to A_R; the slight deviations from the straight lines in the case of $b = 200$ m are likely due to the situation that the value of ϕ_i at the harbour entrance becomes less uniform when the width of the harbour b increases.

The linear relations in figure 12 suggest that except the fundamental standing wave, other wave components inside the harbour may escape the harbour directly without being partially reflected by the sudden widening at the entrance. Even if these waves could be

partially reflected, the proportion of them which are reflected at the entrance should be independent of the length of the harbour, otherwise the relation between A_R and B or B' could not possibly be linear for different values of l. Thus the energy trapping *rate* by the harbour cannot be reinforced by an adjustment of the phase of various waves inside and outside the harbour through a change of l. Therefore, the harbour resonances may not be attributed to the trapping of energy by the harbour. This situation will become even clearer in consideration of the analytical solution of Ünlüata & Mei (1973) and Mei (1983).

In their solution, diverging slightly from Mei's (1983) notation, the surface displacement ζ_d, which can be related to ϕ_d by (4.2), can be written as

$$\zeta_d = \frac{\omega Q}{2g} H_0^{(1)}(kr) e^{-i\omega t}, \tag{6.6}$$

where

$$\frac{\omega Q}{2g} = \frac{-A_0 i(kb/2) \sin kl}{\cos kl + (kb/\pi) \sin kl \ln(\gamma kb/\pi e) - i(kb/2) \sin kl} \tag{6.7}$$

and $H_0^{(1)}$ is a Hankel function of the first kind and r the distance coordinate in figure 1. In (6.7), since normal incidence is under consideration, A_0 stands for the amplitude of the standing wave at the shoreline resulting from a combination of the incident wave and the reflected wave by the seawall. The above solution characteristic of matched asymptotics is valid in the region far from the harbour entrance (the solution in the vicinity of harbour entrance has also been derived simultaneously in Mei (1983)), but the effects of the harbour on this solution have been taken into account by the parameter Q as its magnitude represents the discharge rate from a source at the origin and therefore approximates to the amplitude of the discharge rate per unit depth through the harbour entrance (see Mei 1983, §5.6 for details).

Since the quantity $|\omega Q/2g|$ is essentially proportional to the amplitude of the radiated waves at each point far from the harbour entrance and is independent of the locations, this quantity will be related to the oscillations inside the harbour, which in terms of the total surface displacement has the solution

$$\zeta = \frac{A_0 \cos k(x + l)}{\cos kl + (kb/\pi) \sin kl \ln(\gamma kb/\pi e) - i(kb/2) \sin kl} e^{-i\omega t} \tag{6.8}$$

(see (6.18) in §5.6.2 in Mei (1983)). From (6.6)-(6.8) it is immediately clear that when $kl = n\pi$, the disturbance ζ_d in (6.6) vanishes completely and in the meantime the solution (6.8)

22

has an antinode at the entrance $x = 0$ with the amplitude equal to A_0. Thus a fundamental standing wave inside the harbour can also be seen in this analytical solution. Therefore one may again expect that when $kl \neq n\pi$, the quantity $|\omega Q/2g|$ might be related to the difference between the overall standing wave and the fundamental one in the harbour. This difference can still be represented by two wave trains propagating in opposite directions with different amplitudes, which can also be estimated by using (6.4) and (6.5).

In this case, it follows from (6.8) that at $t = 0$ and in terms of ζ_d instead of ϕ_d,

$$A_P = A_0 \left\{ [\cos kl + (kb/\pi) \sin kl \ln(\gamma kb/\pi e)]^2 + [(kb/2) \sin kl]^2 \right\}^{-1/2}, \tag{6.9}$$

$$\beta = \tan^{-1} \left\{ (kb/2) \sin kl / [\cos kl + (kb/\pi) \sin kl \ln(\gamma kb/\pi e)] \right\} \tag{6.10}$$

and since without the disturbance ζ_d, the standing wave outside the harbour is $\zeta = A_0 \cos kx$ at $t = 0$, we have $\alpha = 0$ at this instant. Therefore, for $\omega = 2\pi/160$ rad sec^{-1} and in the water of 15 m deep, by using the analytical solution and by substituting different values of l, we obtain figures 13 and 14, which are very similar to figures 10 and 12 respectively.

In figure 14, the results for $b = 200$ m can fit a straight line as perfectly as those for $b = 50$ m, because in the present case with normal incidence, the fundamental standing wave inside the harbour can exactly balance the standing wave outside the harbour at the entrance.

Apart from the sample results shown in figures 13 and 14, the expressions (6.9) and (6.10) for A_P and β can be substituded into (6.4) and (6.5) to obtain the expressions for B and B'. On the other hand, the expression for $|\omega Q/2g|$ can easily be obtained from (6.7). Comparison between these results yields

$$\left| \frac{\omega Q}{2g} \right| = kb[(1 + kb/2)^2 + (kb/\pi)^2 \ln^2(\gamma kb/\pi e)]^{-1/2} B, \tag{6.11}$$

$$\left| \frac{\omega Q}{2g} \right| = kb[(1 - kb/2)^2 + (kb/\pi)^2 \ln^2(\gamma kb/\pi e)]^{-1/2} B' \tag{6.12}$$

exactly.

The absence of the term kl from (6.11) and (6.12) ensures a linear relation between $|\omega Q/2g|$ and B or B' for a fixed value of kb. Furthermore, from (6.11) and (6.12) we also have

$$\left| \frac{\omega Q}{2g} \right| = kb(B + B')/2$$

or

$$|Q| = \frac{gk}{\omega} b(B + B')$$ (6.13)

approximately (but exactly when $kb \to 0$). Since the right-hand side of (6.13) represents the largest possible value of the volume flux (or discharge) per unit depth through the harbour entrance induced by the waves ϕ_{out} and ϕ_{in} in (6.3) (because the fluxes due to ϕ_{out} and ϕ_{in} individually may be out of phase), these waves are unlikely to be partially reflected significantly at the entrance, otherwise the above relation cannot be sustained even approximately (because the components reflected at the entrance, like the fundamental standing wave, will make no contribution to the volume flux through the entrance and therefore to $|Q|$). Thus it now becomes clear that the harbour resonances excited by the waves outside the harbour through the entrance are not due to the reinforcement of the energy trapping by harbours, but due to large incoming and outgoing energy fluxes through the entrance. The latter however cannot be seen by inspection of the water surface oscillations in the vicinity of the harbour entrance, because in this region, when the harbour resonates, a node of a standing wave always occurs. This is also the reason why a large amount of incident wave energy can be diffracted through the entrance into the harbour as it is required to relieve a rapid change of the wave field from a node to antinodes on either side of the entrance.

Acknowledgments

References

Abramowitz, M. & Stegun, I. A. 1972 *Handbook of Mathematical Functions* . Dover, New York.

Eckart, C. 1951 Surface waves on water of variable depth. Wave Rep. 100, Scripps Inst. of Oceanogr., Univ. of California, La Jolla.

Green, T. III 1986 Edge waves near a seawall. *Coastal Eng.* **10**, 119-125.

Huntley, D. A., Guza, R. T. & Thornton, E. B. 1981 Field observations of surf beat, 1. progressive edge waves. *J. Geophys. Res.* **86**, 6451–6466.

Hwang, L.-S. & Tuck, E. O. 1970 On the oscillations of harbours of arbitrary shape. *J. Fluid Mech.* **42**, 447–464.

Kane, J. H. 1994 *Boundary Element Analysis in Engineering Continuum Mechanics* . Prentice Hall, Englewood Cliffs, New Jersey, USA.

Lee, J.-J. 1971 Wave-induced oscillations in harbours of arbitrary geometry. *J. Fluid Mech.* **45**, 375–394.

Mei, C. C. 1978 Numerical methods in water-wave diffraction and radiation. *Ann. Rev. Fluid Mech.* **10**, 393–416.

Mei, C. C. 1983 *The Applied Dynamics of Ocean Surface Waves*. Wiley-Interscience, New York.

Mei, C. C. & Agnon, Y. 1989 Long-period oscillations in a harbour induced by incident short waves. *J. Fluid Mech.* **208**, 595–608.

Mei, C. C. & Chen, H. S. 1975 Hybrid element method for water waves. *Symp. on Modeling tech.* 2nd Annual Symposium of the Waterways Harbors and Coastal Engineering Division, ASCE, **1**, 63-81.

Miles, J. & Munk, W. 1961 Harbor paradox. *Proc. Am. Soc. Civ. Engrs., J. Waterways Harbors Div.* **87**, 111-130.

Neu, W. L. & Oh, I. 1987 Edge waves on linear segmented Topographies. *Proc. Coastal Hydrodyn.* Newark, Delaware, 227–240.

Schäffer, H. A. & Jonsson, I. G. 1992 Edge waves revisited. *Coastal Eng.* **16**, 349–368.

Ünlüata, Ü & Mei, C. C. 1973 Long wave excitation in harbors—an analytic study. Dept. of Civ. Engrg. M.I.T. T.R. no. 171.
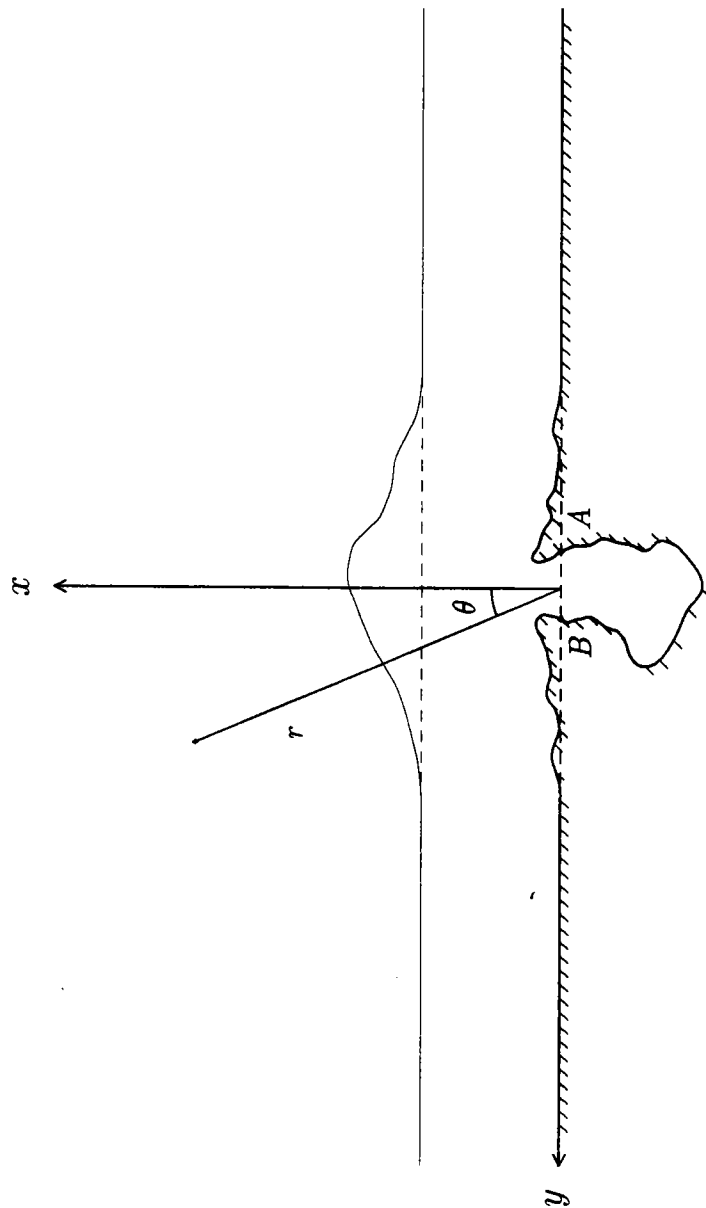
Figure 1. Definition sketch. The narrow solid line represents the division between the sloping beach and the horizontal shelf.
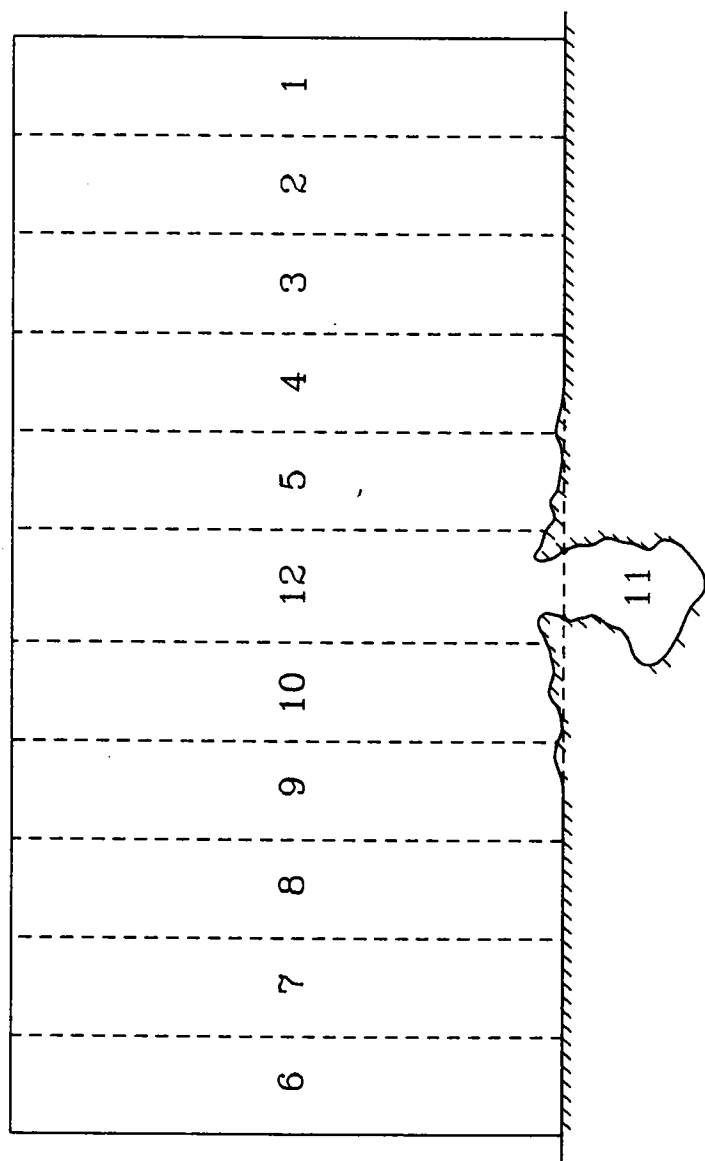
Figure 2. Domain broken into portions.
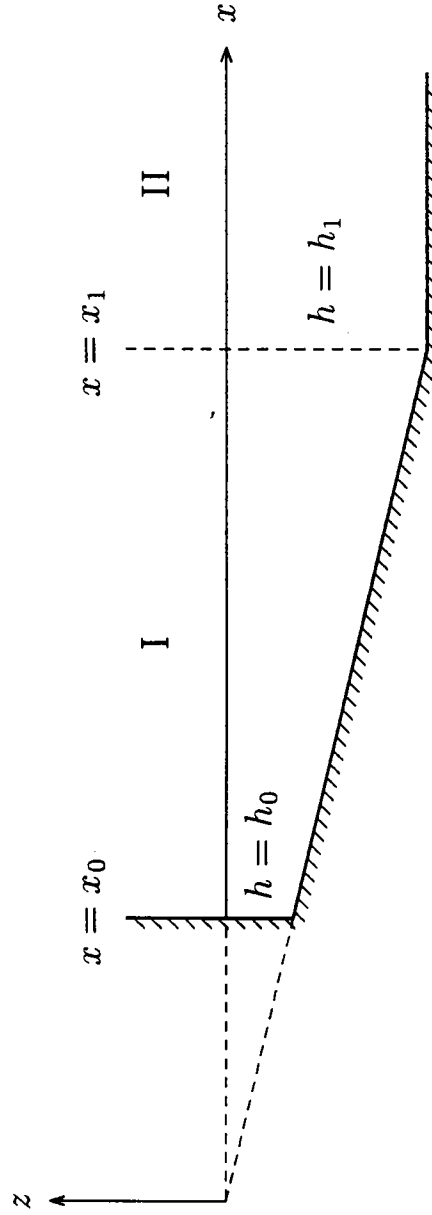
Figure 3. Cross-section of a plane sloping beach with a vertical seawall and a horizontal shelf.
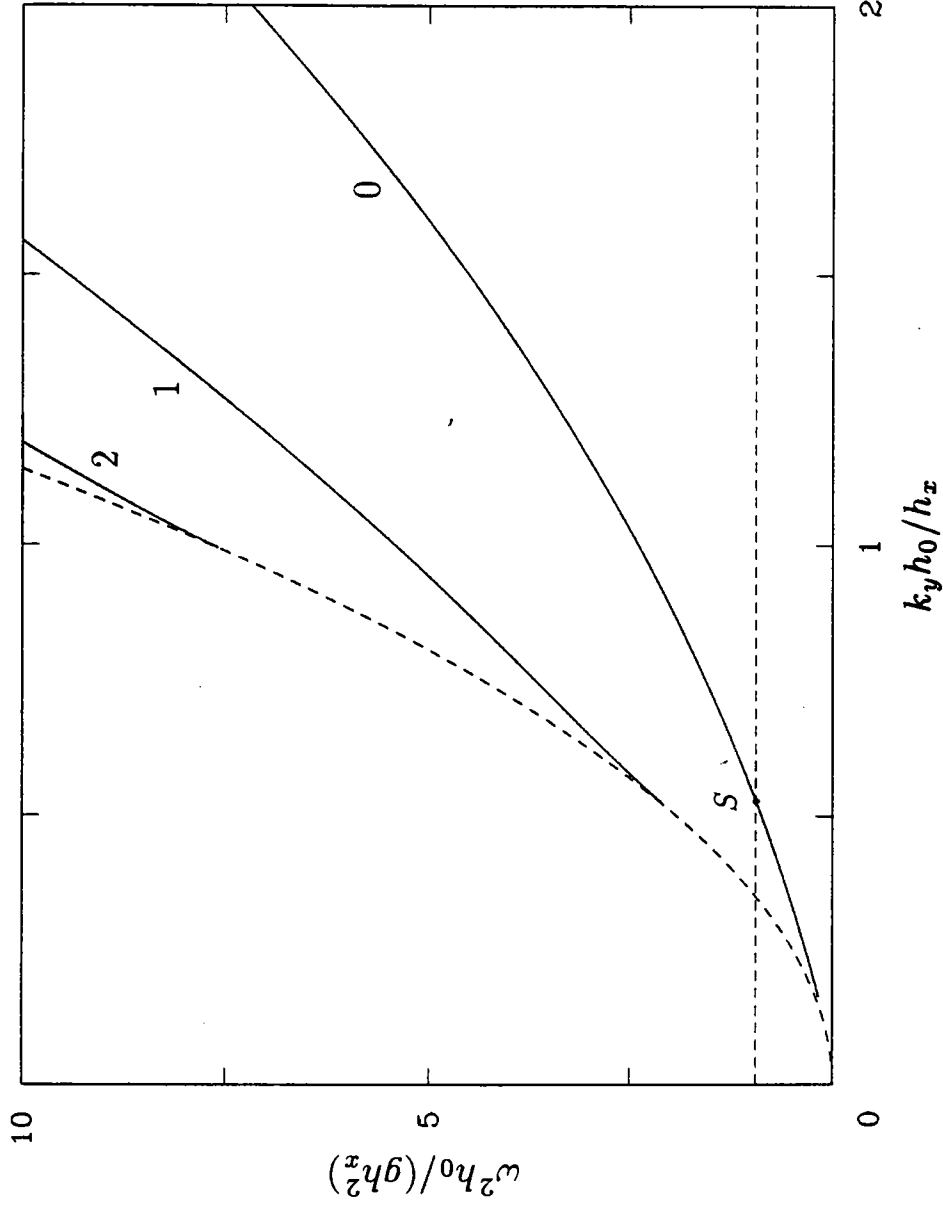
Figure 4. The dispersion relation of edge waves for the topography shown in figure 3. The broken curve indicates $\lambda = 0$ and therefore represents a cut-off of the frequency when $h_0 = 15$ m, $h_1 = 115$ m, and $h_x = 0.05$. The horizontal line indicates $\omega = 2\pi/160$ rad sec^{-1}, which intersects only the first solid curve (representing the fundamental mode) at $k_y = 0.001764$ rad m^{-1}.
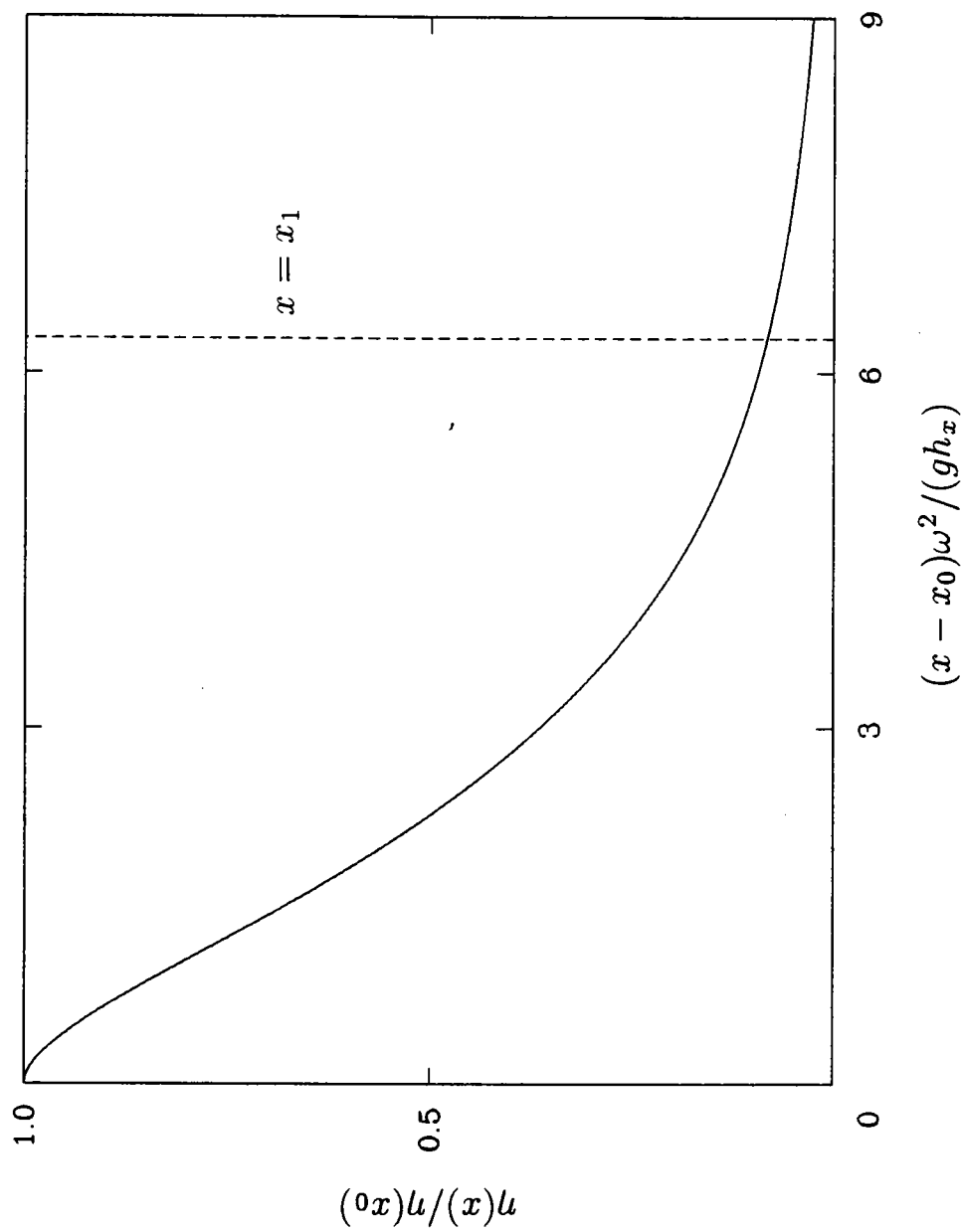
Figure 5. Profile of the fundamental edge wave mode under the circumstances corresponding to point S in figure 4.

Figure 6. The domain and boundary of the numerical computations. The horizontal broken line represents the division between the sloping beach and the horizontal shelf.
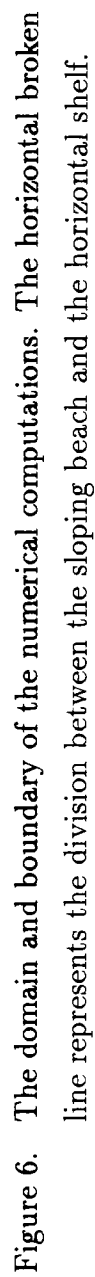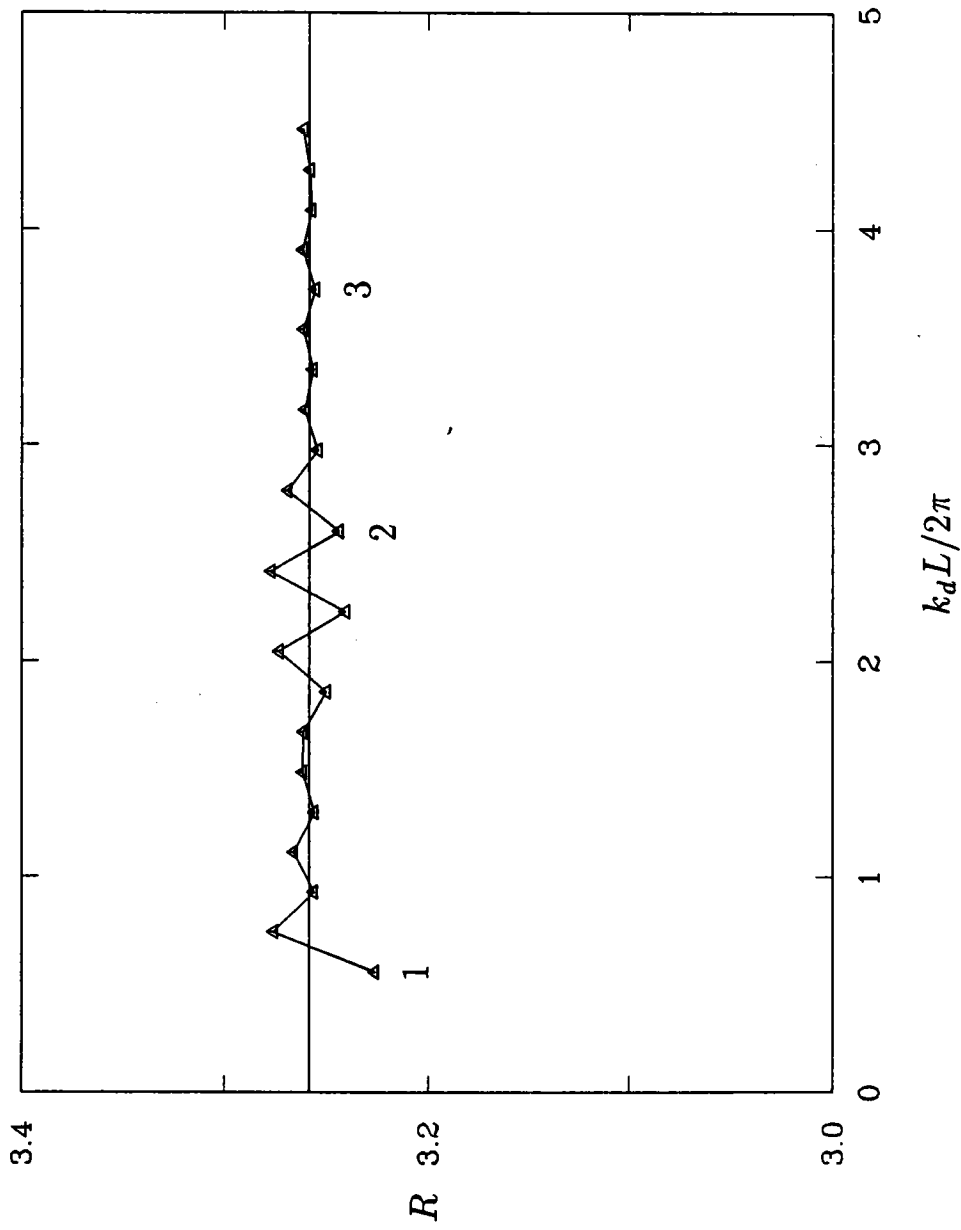
Figure 7. A convergence test of the numerical solutions. The horizontal line indicates the mean value of the results.
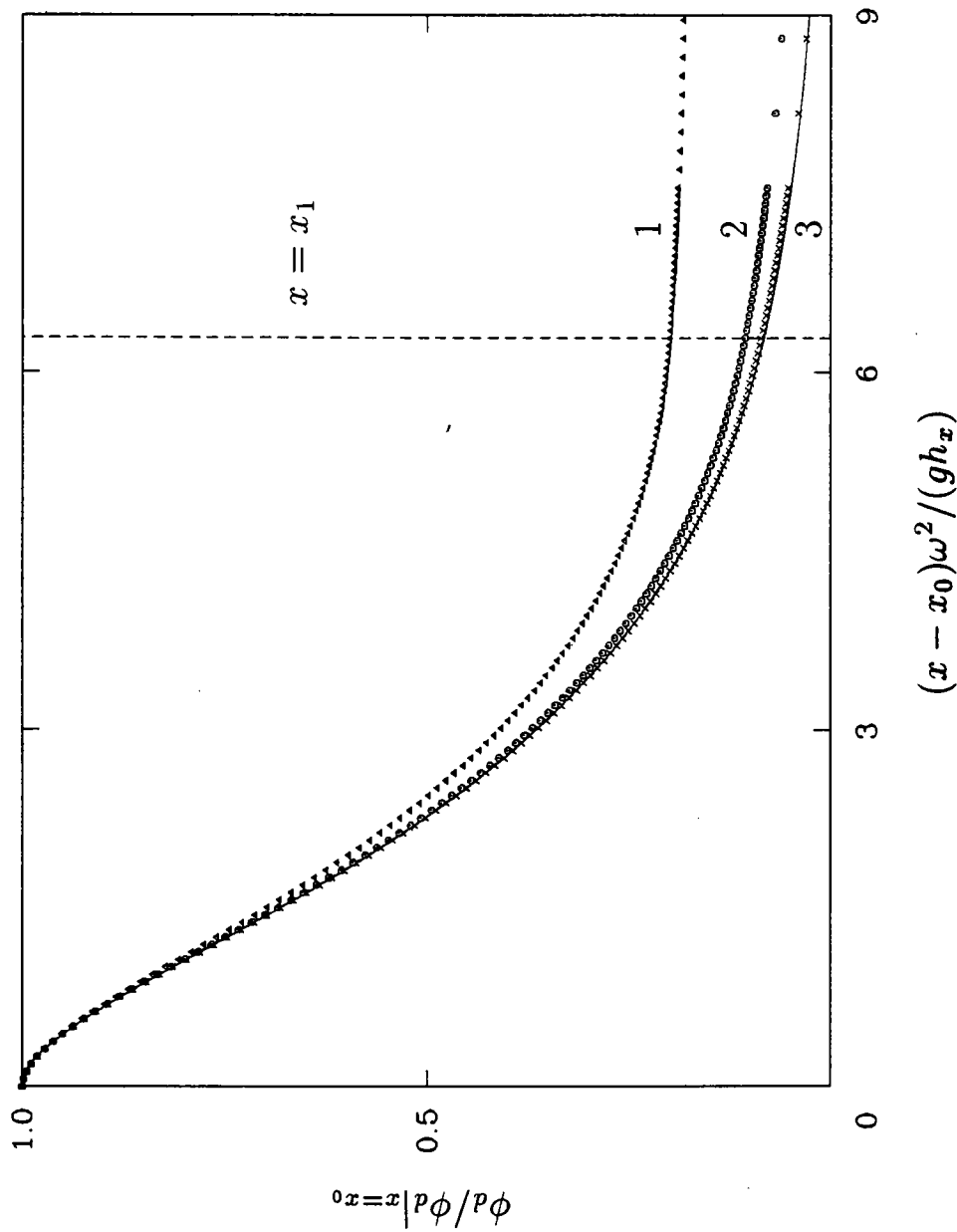
Figure 8. The comparison between the numerical and analytical solutions of the edge wave profile. The curve is identical with that in figure 5. The groups of the data points labeled by 1, 2, 3 represent the numerical solutions under the circumstances corresponding to those of the data points in figure 7 with the same labels.
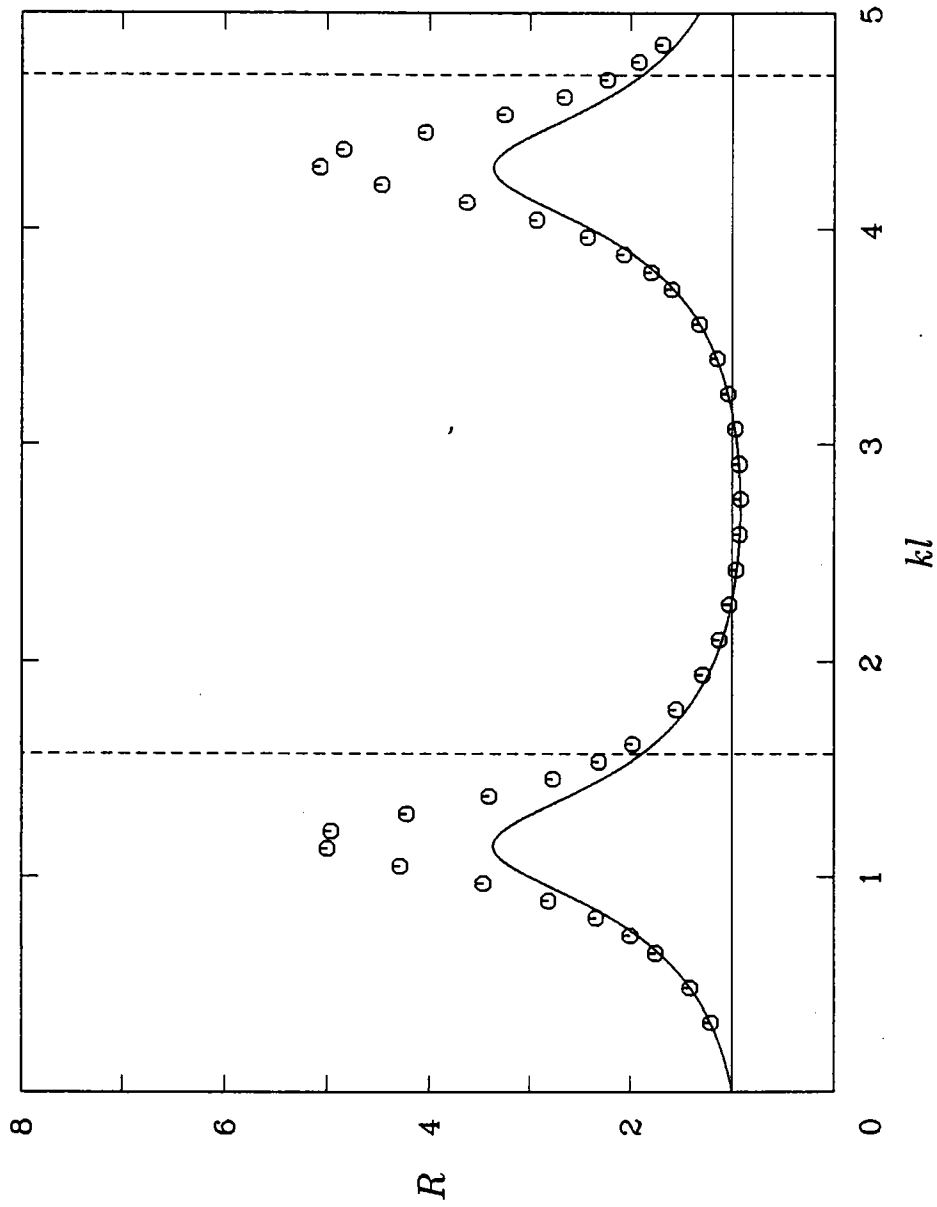
Figure 9. Variation of the amplification factor for (a) $b = 200$ m and (b) $b = 50$ m. The circles represent the present numerical solutions. The curve is the analytical solution of Ünlüata & Mei (1973) and Mei (1983). The broken lines indicate the locations where $kl = \pi/2$ and $kl = 3\pi/2$, and the horizontal line the location of $R = 1$.

(b)
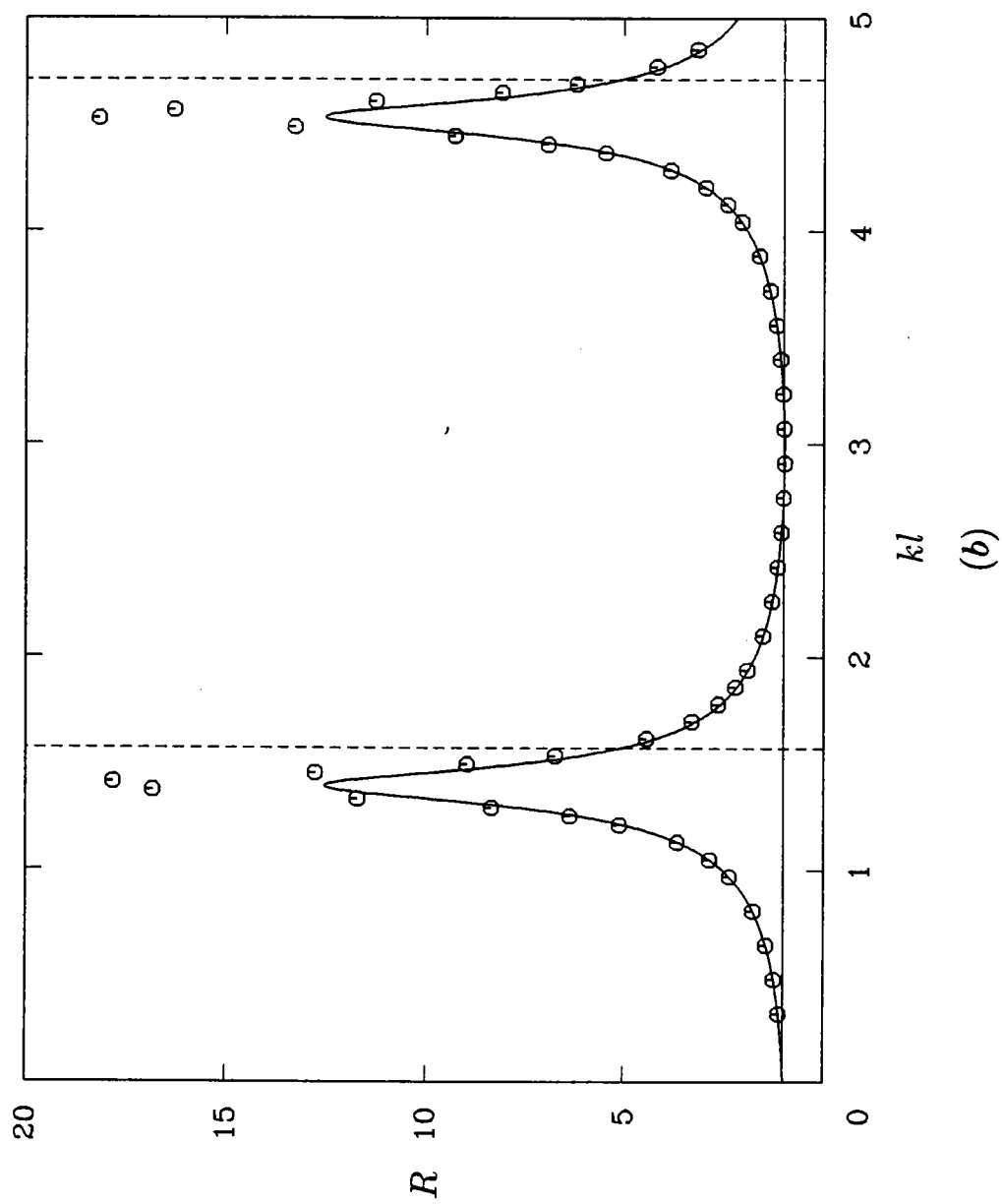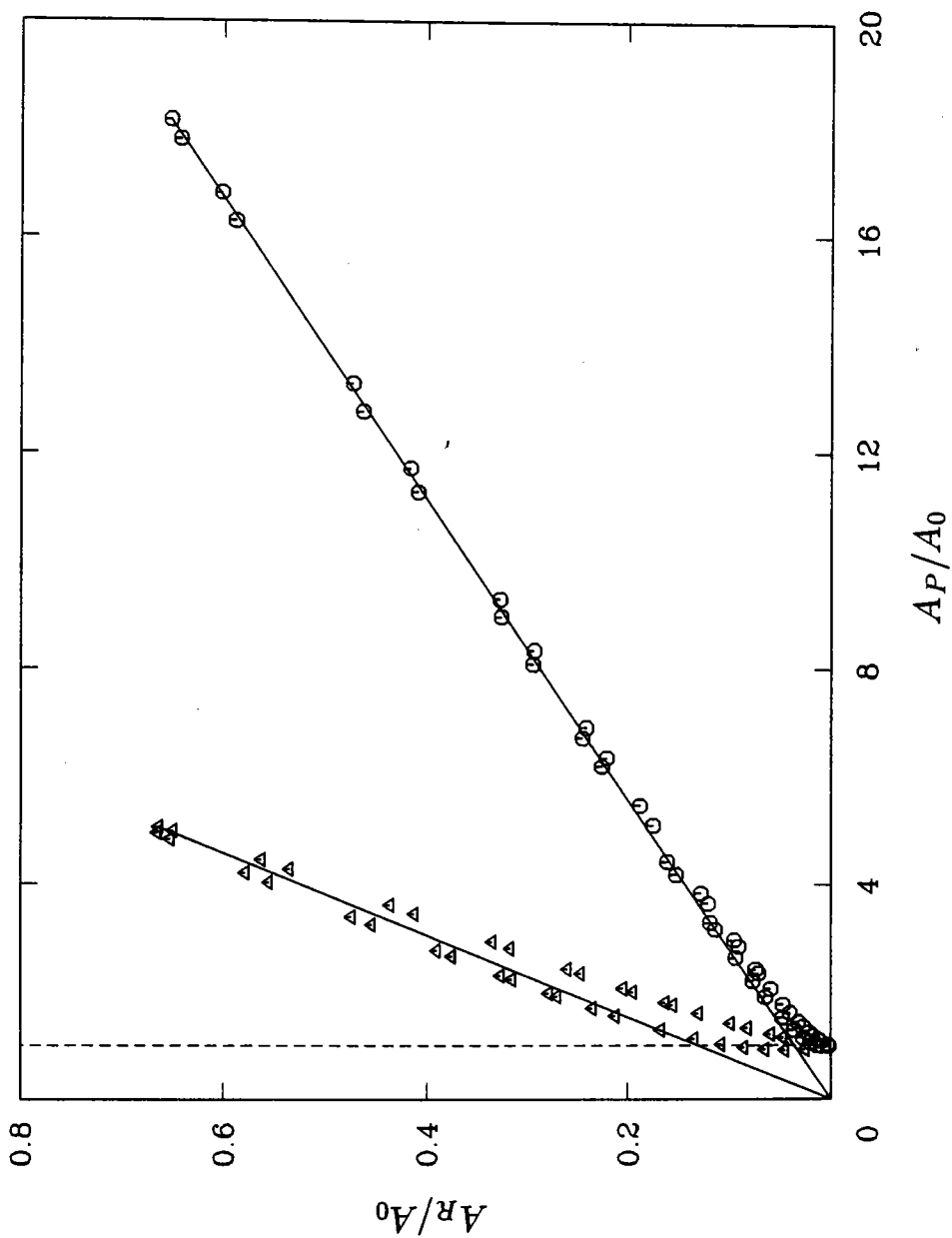
Figure 10. The relation between A_R and A_P for $b = 200$ m (triangles) and $b = 50$ m (circles). Solid lines are the straight lines passing through the origin and the data points with the largest value in each case. The broken line indicates the location of $A_P/A_0 = 1$.
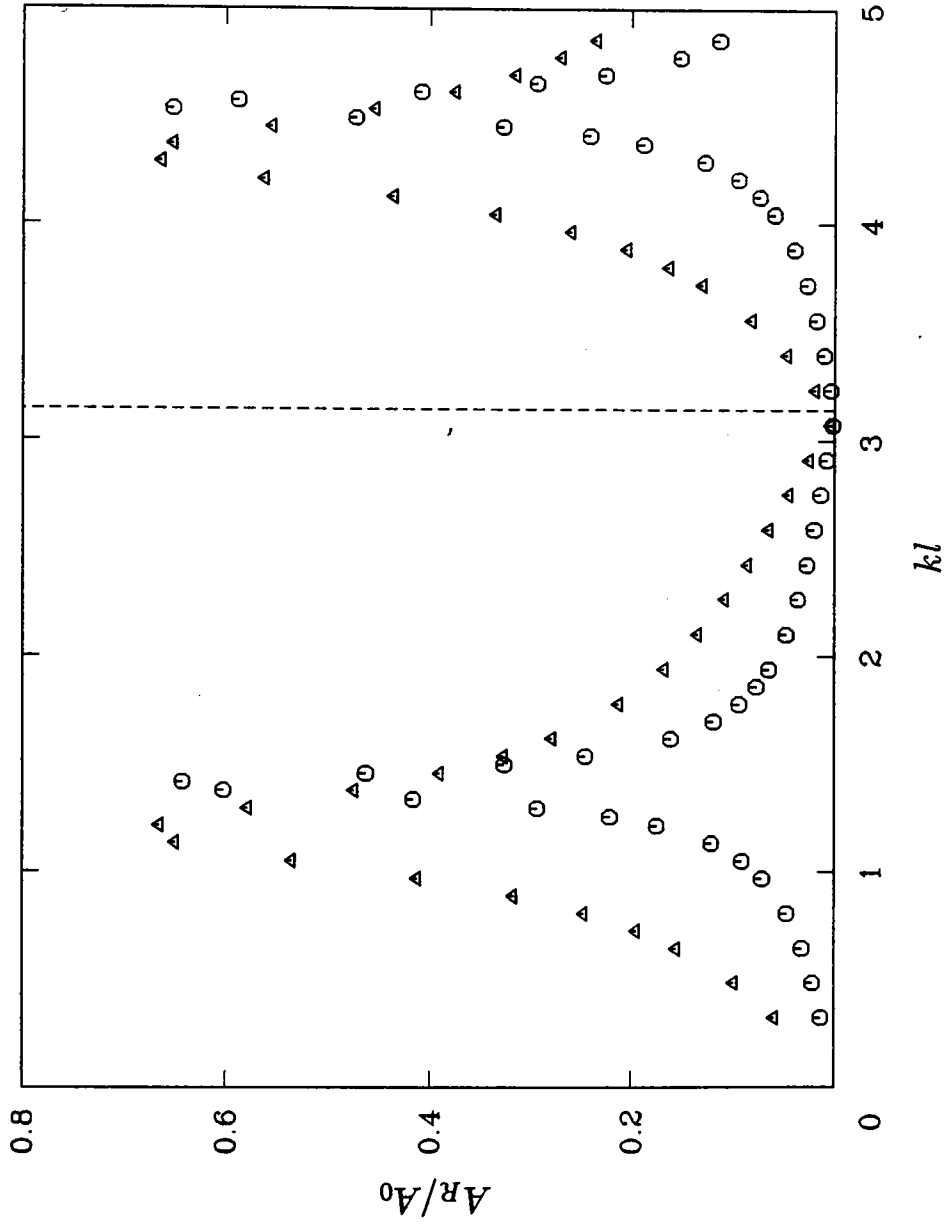
Figure 11. Variation of A_R/A_0 with kl for $b = 200$ m (triangles) and $b = 50$ m (circles). The broken line indicates the location of $kl = \pi$.
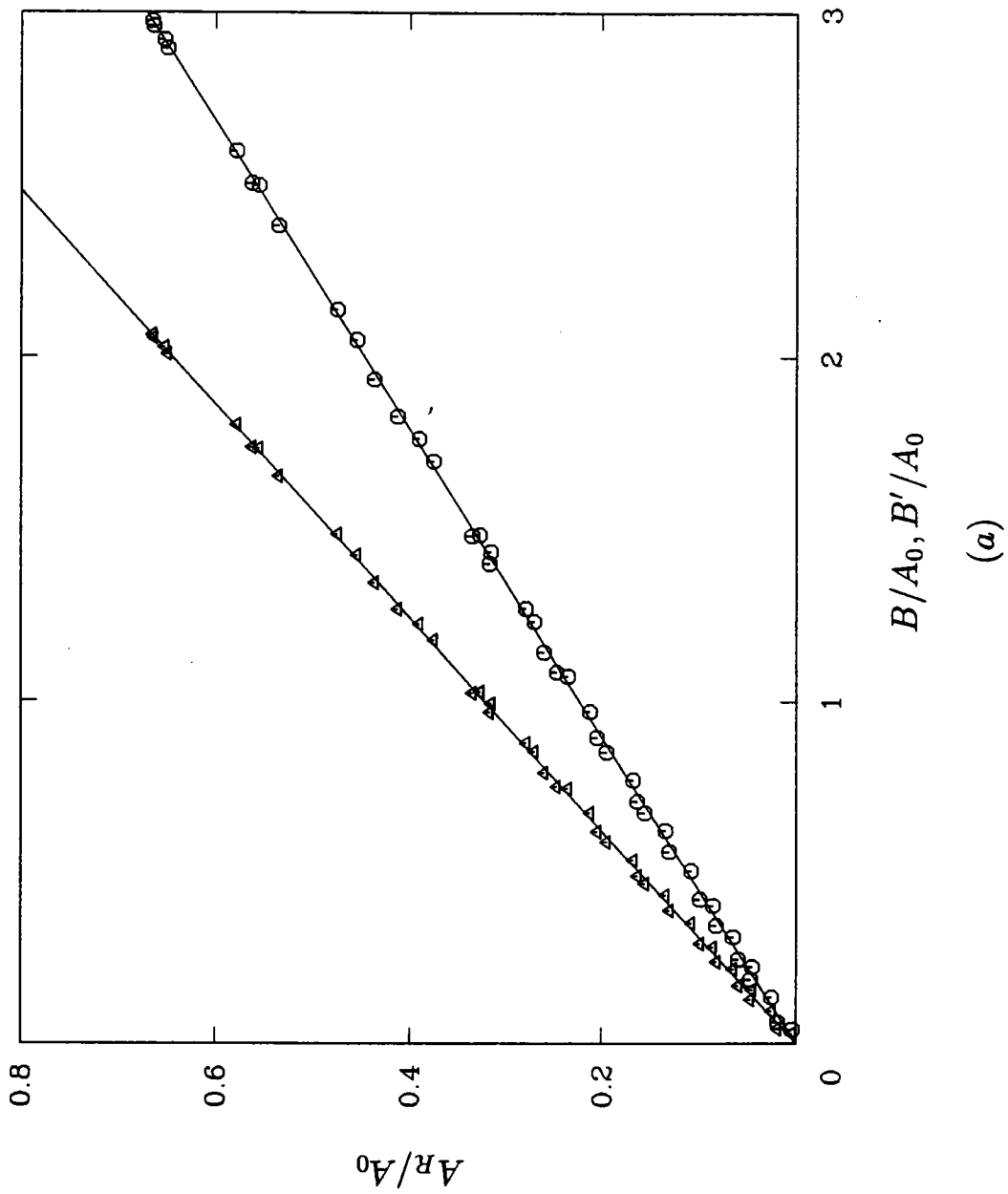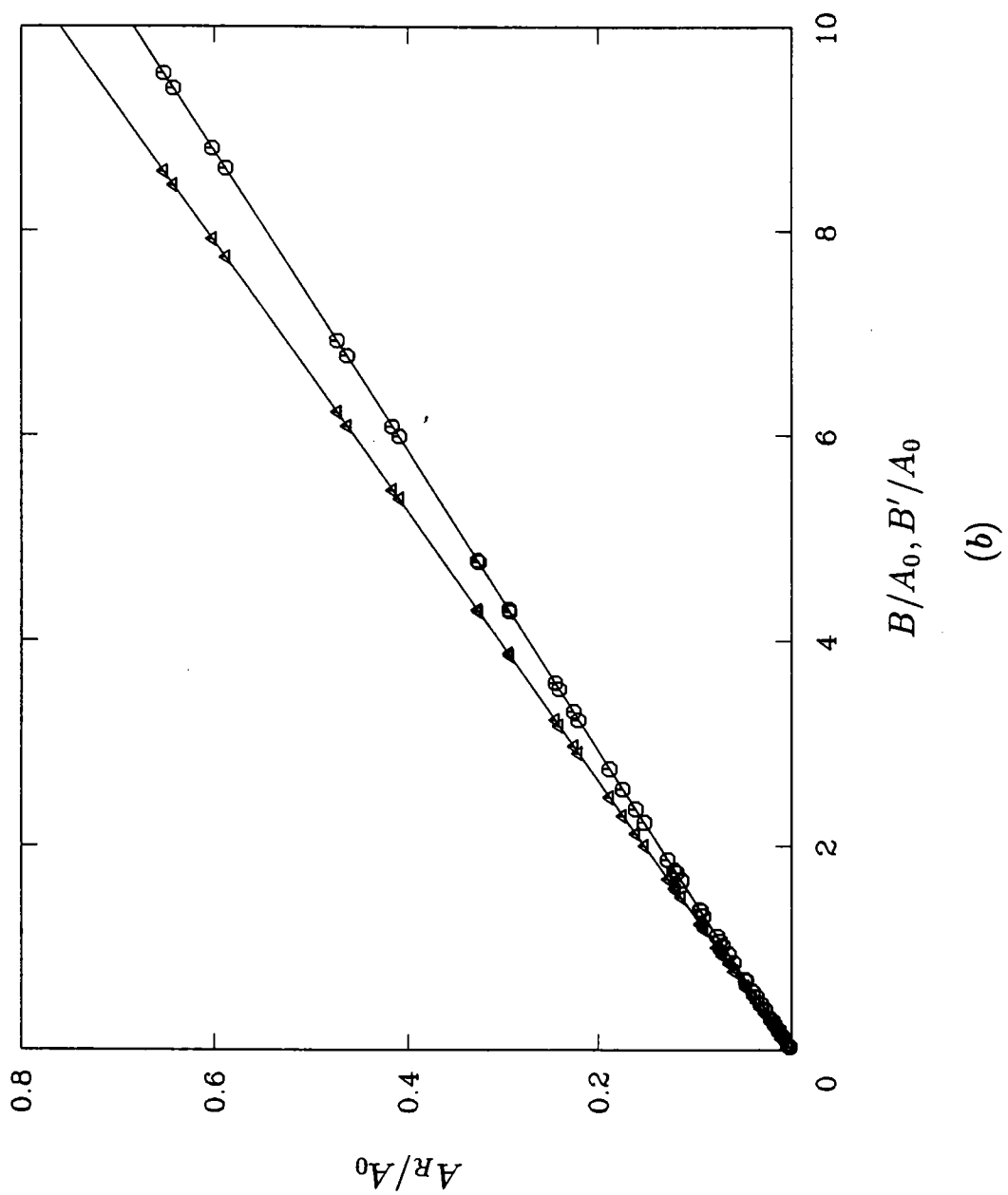
Figure 12. The relations between A_R and B (circles) and between A_R and B' (triangles) for (a) $b = 200$ m and (b) $b = 50$ m. Solid lines are the best fit straight lines constrained to pass through the origin.
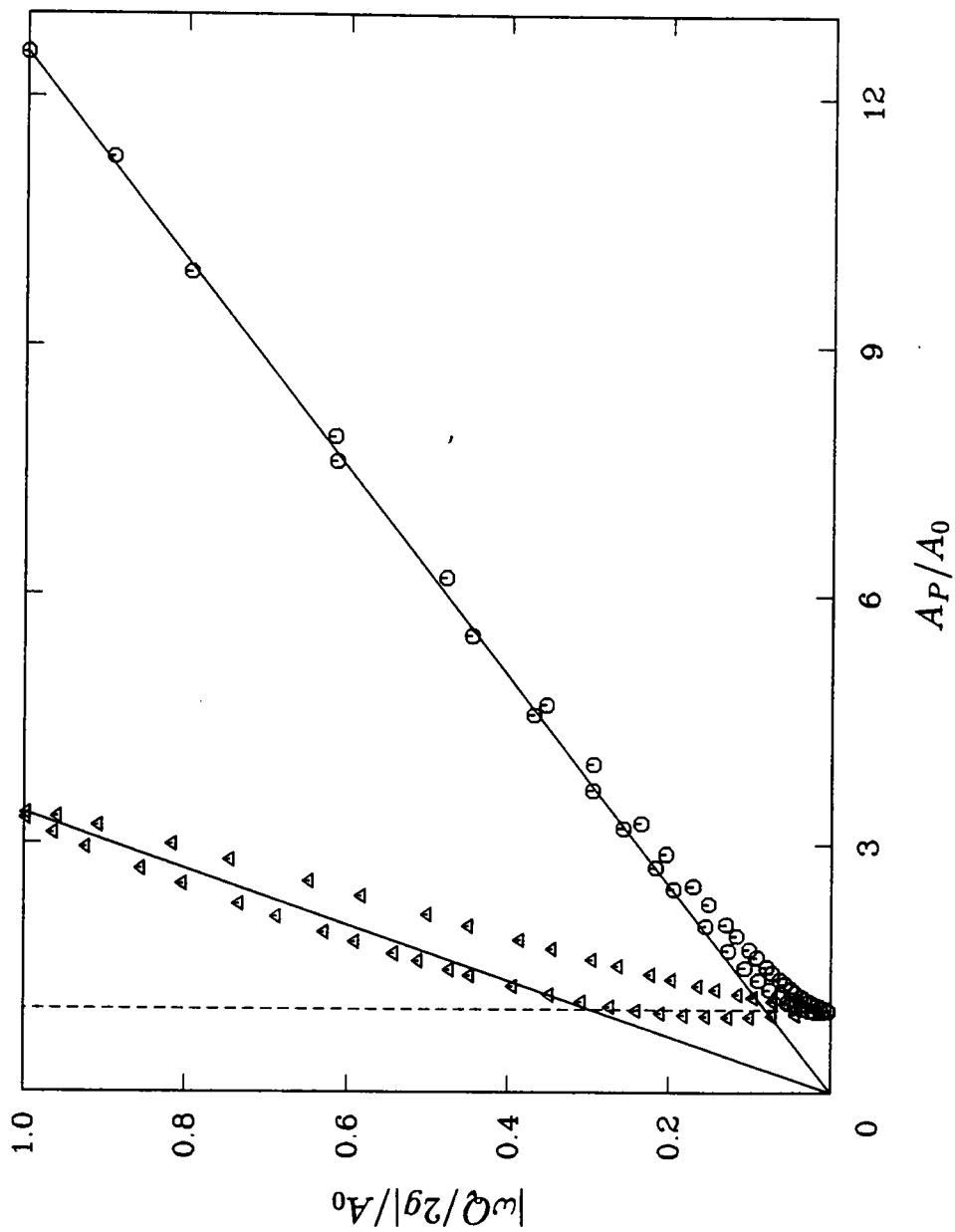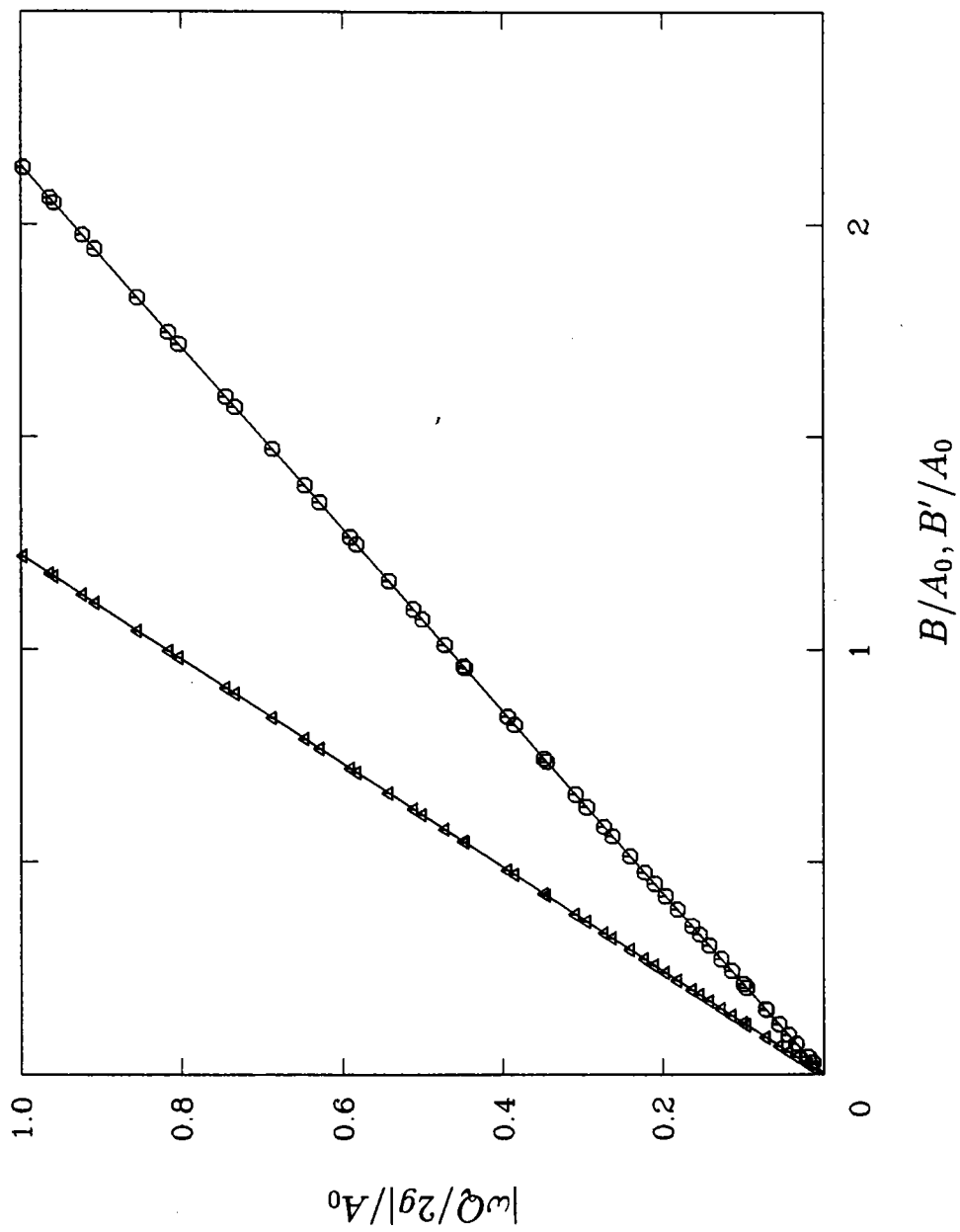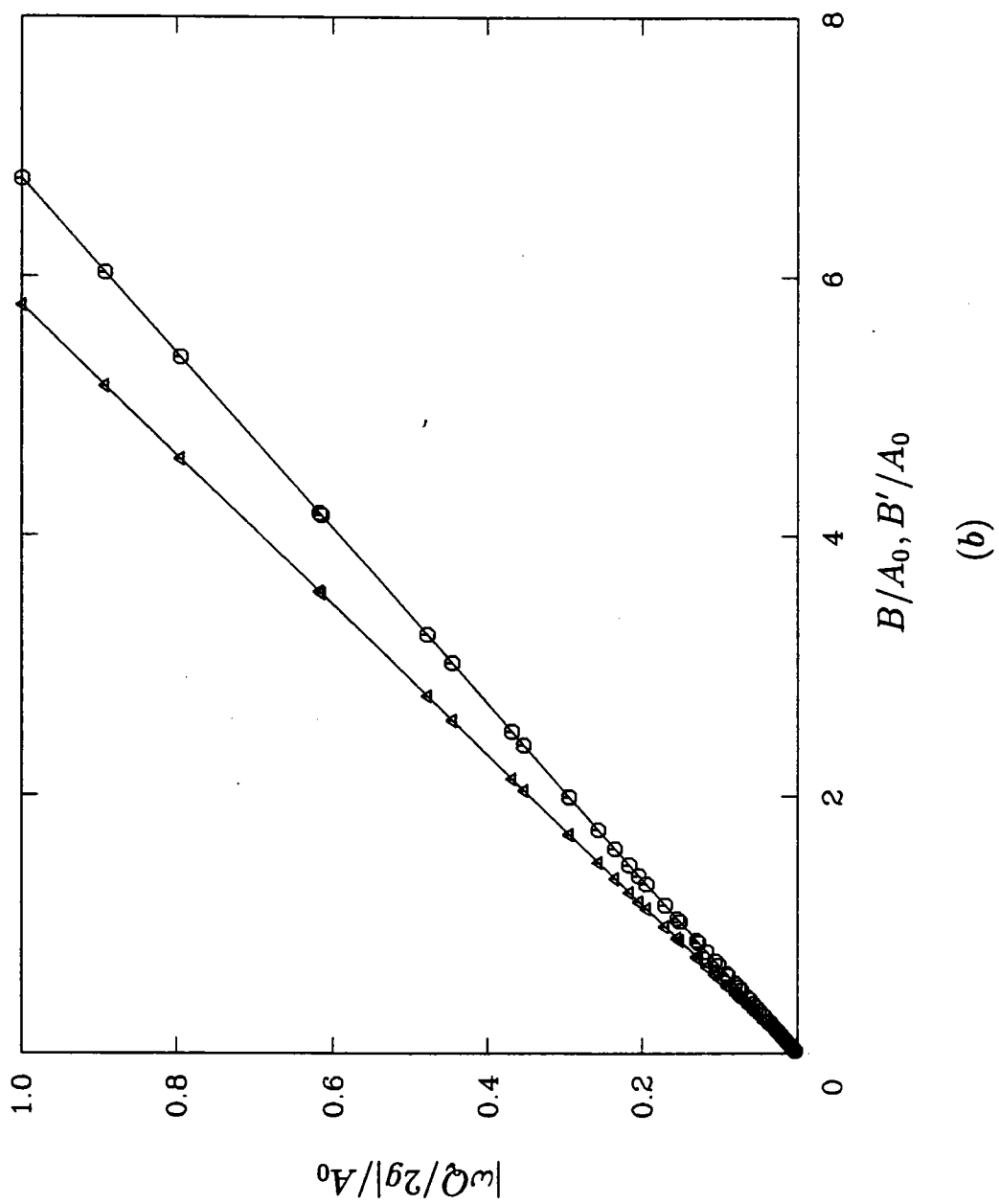
(b)

Figure 13. The relation between $|\omega Q/2g|$ and A_P for $b = 200$ m (triangles) and $b = 50$ m (circles). Solid lines are the straight lines passing through the origin and the data points with the largest value in each case. The broken line indicates the location of $A_P/A_0 = 1$.

Figure 14. The relations between $|\omega Q/2g|$ and B (circles) and between $|\omega Q/2g|$ and B' (triangles) for (a) $b = 200$ m, (b) $b = 50$ m. Solid lines are the best fit straight lines constrained to pass through the origin.

(b)